J Clin Monit Comput (2017) 31:19–41
DOI 10.1007/s10877-016-9830-z

REVIEWPAPER

Using the features of the time and volumetric capnogram for classification and prediction

Michael B. Jaffe[1]

Received: 29 July 2015 / Accepted: 6 January 2016 / Published online: 18 January 2016

Abstract Quantitative features derived from the time-based and volumetric capnogram such as respiratory rate, end-tidal PCO_2, dead space, carbon dioxide production, and qualitative features such as the shape of capnogram are clinical metrics recognized as important for assessing respiratory function. Researchers are increasingly exploring these and other known physiologically relevant quantitative features, as well as new features derived from the time and volumetric capnogram or transformations of these waveforms, for: (a) real-time waveform classification/anomaly detection, (b) classification of a candidate capnogram into one of several disease classes, (c) estimation of the value of an inaccessible or invasively determined physiologic parameter, (d) prediction of the presence or absence of disease condition, (e) guiding the administration of therapy, and (f) prediction of the likely future morbidity or mortality of a patient with a presenting condition. The work to date with respect to these applications will be reviewed, the underlying algorithms and performance highlighted, and opportunities for the future noted.

Keywords Capnography · Prediction · Classification · Detection · Screening · Feature extraction

✉ Michael B. Jaffe
mbjengineering@cox.net

[1] Cardiorespiratory Consulting, LLC, 410 Mountain Road, Cheshire, CT 06410, USA

1 Introduction

The measurement of carbon dioxide in the breath using chemical absorption and infrared methods dates to the mid-nineteenth century [1, 2]. These early methods provided mixed expired estimates from the collected expiratory gas, and their potential applicability to clinical care was recognized in the "popular" scientific literature of the time [3]. In the early twentieth century, researchers explored the nature of the expiratory carbon dioxide curve, including the physiologic components (e.g. dead space, alveolar gas etc.), and the shape of the time and volumetric waveform with methods such as rapid sequential gas volume sampling [4]. However, it was not until the widespread commercial availability of rapid infrared analyzers that the determination of the partial pressure of carbon dioxide in the breath was able to move from the physiology research lab to the "bedside" [5]. This technology initially found application in anesthesia and later in critical care for a limited number of uses, and only recently has its application spread to other clinical environments and evolved to new clinical uses [6].

It was in the mid to late 1950s that investigators began to apply manual and electronic computational approaches to the fitting of the carbon dioxide and flow curves (i.e. time and volumetric capnogram) and estimation of parameters, such as alveolar PCO_2 and ventilation [7]. This was initially undertaken with manual time-consuming methods (e.g. [8]) that were soon supplemented by analog computers [7], combined analog/digital computers [9] (Fig. 1), and, later, with expensive and complex digital computers [10].

The early capnographs relied on analog electronic methods to determine the parameters of respiratory rate (RR) and end-tidal partial pressure of CO_2 ($P_{ET}CO_2$). The

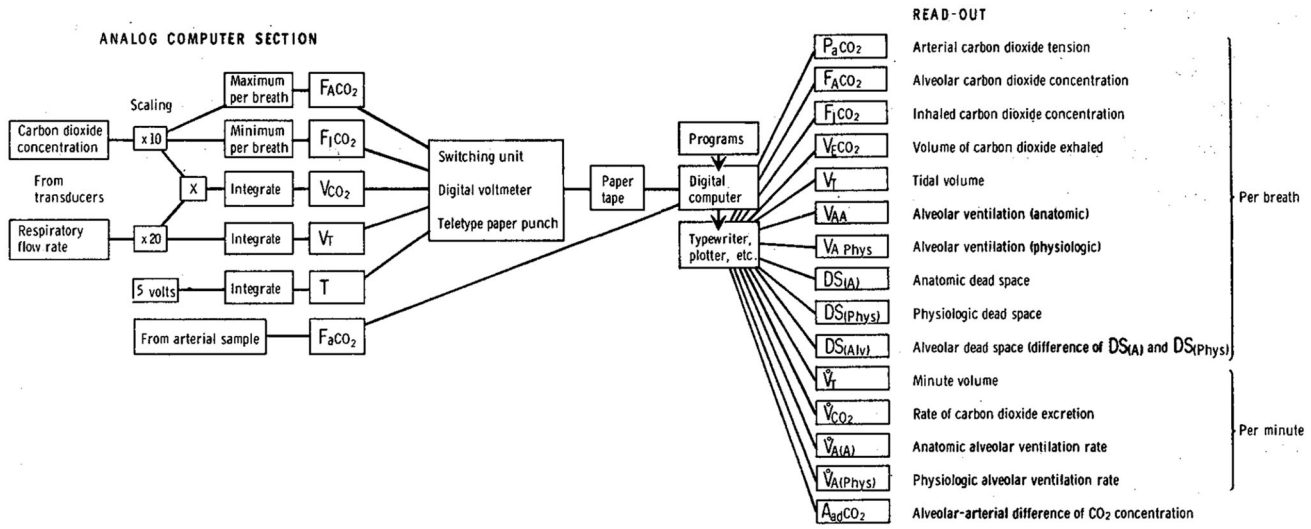

Fig. 1 Computation of time and volumetric capnographic features using a combined analog/digital computer with the digital output of the analog system transferred to the digital computer (CDC 160A 12-bit minicomputer, Control Data Corporation) with a punched paper tape (©ACM. Reprinted with permission from AFIPS-FJCC'65. Murphy [9])

introduction of the microprocessor in the early 1970s led to software-based measurements of respiratory rate and $P_{ET}CO_2$, with one manufacturer integrating CO_2 and volume to calculate alveolar ventilation and carbon dioxide elimination [11]. However, despite the application by investigators of computing technology to identify and classify real-time changes in the capnogram in the late 1980s (e.g. [12–14]), the software algorithms in currently available commercial devices still do not offer this capability, and remain focused on robust estimation of respiratory rate, end-tidal measurements, and novel indices.

With $P_{ET}CO_2$ and RR typically computed for clinical use from the time-based carbon dioxide waveform (capnogram), it was widely understood that the shape of the waveform and trend data conveyed important clinical information about the state of the patient and equipment. Despite descriptions in the literature of the shape of normal and obstructive capnograms dating back to the early 1960s [15], there remains no widely accepted standard methodology or library of waveforms to differentiate between normal and abnormal capnograms as currently exists for some of the other physiologic signals (e.g. MIT database for ECG). Prof. Bob Smalhout, an early proponent of capnography[1] published the classic, *Atlas of Capnography* [16]. This atlas consisted of over 20 sections of annotated waveforms of CO_2 versus time strip chart tracings that were derived from his collection of about 6000 manually annotated capnograms. Later publications added to this work with annotated waveforms from neonates [17] and mechanically ventilated children [18]. For the last 50 years, the clinical identification of abnormal waveforms, and changes of those waveforms, was primarily based on the visual skill of the observer and, if available, the use of paper waveform wall charts (e.g. Novametrix Medical Systems) or monitor-embedded waveform libraries (Teach Mode in Model 1260 & 7000, Novametrix Medical Systems) [19].

With the growing clinical use of capnography driven in part by clinical standards and guidelines in anesthesia and critical care, researchers began to study the capnogram's value for screening for disease, detecting abnormal conditions, predicting mortality or values of invasively determined parameters, and classifying patients into groupings, such as normal, CHF or COPD, based on features from the capnogram alone and in combination with other measurements. Those studies included using single or averaged values of the $P_{ET}CO_2$ values as a surrogate for arterial CO_2 [20] and as a predictor of survival during CPR [21], as well as changes in end-tidal CO_2 to determine changes in clinical condition (e.g. sudden pulmonary embolism) [22]. New metrics have been defined using the shape or statistical properties of the waveform to distinguish between different disease states [23, 24]. However, leveraging information on the shape of the waveform, with or without contextual information, or in conjunction with a physiologic model to allow easier interpretation, as with the volumetric capnogram, has been limited. Researchers and companies have been exploring the use of capnographic features and learning methods for applications such as classifying patients into one of several classes (e.g. asthma, CHF, normal), predicting success of an action (e.g. extubation, defibrillation during CPR), and classifying waveforms on a real-time basis to detect abnormalities.

In conjunction with the growth of capnography has been the proliferation of supervised learning methods and their

[1] The continuous graphical time tracing of carbon dioxide from the breath.

application to the capnogram for prediction and classification. The features of the capnogram that investigators have explored for use in prediction and classification, and the clinical applications that have leveraged these features and learning methods will be reviewed.

2 The signal and its features

The term, capnogram (i.e. the time-based capnogram), usually refers to the tracing of carbon dioxide over time rather than the volumetric capnogram, which is the tracing of carbon dioxide over volume in which the inspiratory portion of the waveform is usually not shown. Both waveforms are subdivided into three phases (with a fourth for inspiration with the time capnogram) associated with the source of the expiratory gases: (1) gas from the dead space; (2) gas from the transition between dead space and alveolar gas; and (3) gas from sequential emptying of the alveolar volumes (Fig. 2) [26]. From these waveforms and the respective phases, time- or volume-based features, usually with a direct physiologic or clinical basis such as various angles, slopes, normalized slopes, peak values, durations, or volumes of each phase, areas and derived values are commonly computed (Table 1). Note that the terminology used for the phases, the phase transitions, angles, and slopes, is similar for the time and volumetric capnogram; it is important to be careful with their usage, as they are not equivalent.

From the time–based capnogram, estimates of respiratory rate, end-tidal CO_2, and inspiratory levels of CO_2 are usually reported. The most well-known capnographic parameter, the end-tidal carbon dioxide value ($P_{ET}CO_2$), is actually one of the least understood. It is often expected to equate to the arterial value; however, the estimated value depends on how it is measured and calculated, and on the patient's physiology (diffusion, ventilation, cardiac output), with an end-tidal arterial gradient usually present. As the name suggests, end-tidal value refers to the carbon dioxide value at end-expiration. However, in practice, the intent is to provide a value as close as possible to the actual alveolar partial pressure, and other values, such as the highest CO_2 sample value during expiration, are often reported.

The respiratory rate derived from the capnogram is generally determined from the time between the transitions between expiration and inspiration of each breath. On face value, the determination of these transitions seems simple, but, in practice, it can be quite complicated, and obtaining appropriate breath criteria is dependent on the clinical environment and application [27, 28]. Note, however, that to help improve specificity and sensitivity, many manufacturers will apply additional "screening" using algorithms with names such as SARA^{TM} [29] and RENE^{TM} [30].

Inspiratory CO_2 values or the presence of an elevated level of inspiratory CO_2 is typically reported by commercial instruments and used to indicate the presence of rebreathing. Of greater use is the inspired CO_2 volume, a quantitative measure of the amount of rebreathing [31].

Measurements of the angles at the transitions during expiration from phase I to phase II (i.e. take-off angle), from phase II to phase III (i.e. α angle), and from phase III to start of the next inspiration (i.e. β angle) have been determined from the capnogram and used as features for classification. For example, the slopes and volume-normalized slopes of phase II and phase III of the volumetric capnogram have been widely used to determine classification, with a central portion of each phase fitted with a line to represent the respective slope. Additionally, the volumetric capnogram has been further subdivided by volume within each phase [32] and fitted with functions [33] to better and more reliably characterize the waveform and produce derived estimates with greater reproducibility.

Coupling capnography with flow (and volume) measurements allows the estimation of a number of physiologically based and clinically interpretable measures of respiratory function, such as anatomic and physiologic dead space and the associated normalized ratios, CO_2 elimination, and pulmonary capillary blood flow (Table 1). These measures allow insight into many cardiopulmonary disorders, including adult (acute) respiratory distress syndrome, chronic obstructive pulmonary disease, asthma, and pulmonary embolism. Viewing the changes in carbon dioxide as a function of volume, rather than time, allows for interpretation of the reported values, and changes in those values, in a context consistent with known physiologic concepts. This unified physiologic framework, which divides the volumetric capnogram into phases I–III [34], allows for enhanced characterization and interpretation of the volumetric capnogram using a number of derived features (Fig. 2b). One of the features from this framework is a noninvasive surrogate for anatomic dead space, airway dead space, estimated by the equal area Fowler method [35] which uses the fitted "linear" central portions in Phase III (e.g. 40–80 % of expired volume) and Phase II. This measure allows airway dead space to be computed on a breath-to-breath basis for each patient rather than relying on the problematic rule-of-thumb of 1 mL of dead space for every pound of body weight. Brewer et al. [36] found that this rule, derived from population averages, when compared to measured airway dead space, showed no correlation ($r^2 = 0.0002$). Over time, researchers became concerned about the effect of measurement noise on dead space volume estimates from the Fowler method and the resulting variation in these calculated parameters. This led

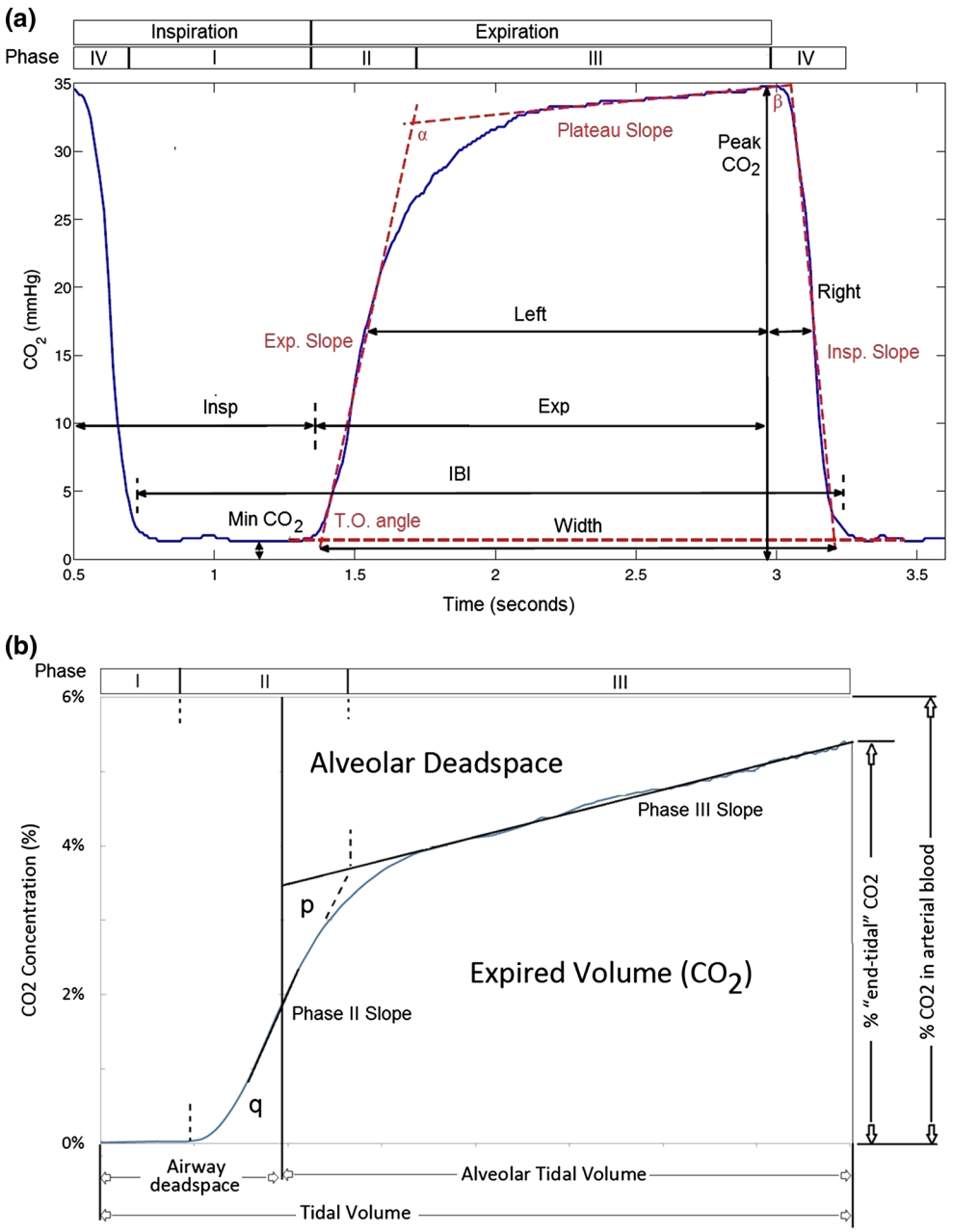

Fig. 2 **a** Time-based capnogram. Inspiratory segment (Phase 0) and expiratory segment (divided into Phases I, II, III,IV) α = angle between Phase II and Phase III (normal range 100° to 110°), β = angle between Phase III and descending limb of Phase 0 (inspiration) (normal approx. 90°), T.O. angle = takeoff angle. (Adapted from Herry et al. [25] © Institute of Physics and Engineering in Medicine. Reproduced by permission of IOP Publishing. All rights reserved.) **b** Volumetric capnogram (CO_2/Volume Plot) (inspiratory portion not shown) divided in 3 phases with volumes and slopes shown (note areas p, q are used to determine airway deadspace via the Fowlers equal area method)

to the development of methods with lower dispersion, which included fitting the expiratory volume of CO_2 versus expiratory volume curve between 40 and 80 % of the expired volume using first, second, and third order polynomials [37]. More recently, it involved fitting the expiratory volumetric capnogram using a functional approximation determined with a non-linear least squares algorithm [33] resulting in decreased intra-patient breath-to-breath variability and dispersion of the calculated parameters.

The features discussed in this section are intended to be interpretable using known physiologic or clinical concepts. Researchers have also explored the unique features of the capnogram for use (Table 2) (Fig. 3) in their learning algorithms that are often more challenging to interpret in a clinical context. These features include

Table 1 Comparison of known features available in volumetric and time-based capnography

Features	Available?		Comment(s)
	Time	Volumetric	
End-tidal CO_2	Yes	Yes	Time-based average—method manufacturer dependent; rebreathing and artifacts complicate calculation
Breathing frequency	Yes	Yes	Upper limit dependent on gas sampling method and technology and clinical situation
Inspiratory/expiratory times	Yes (see comment)	Yes	Time: inspiratory to expiratory transition difficult to reliably measure; Expiratory to inspiratory transition changes with rebreathing Volumetric: determined from flow waveform
Inspired CO_2	Yes	Yes	Time: Minimum value often used Volumetric: Volume of inspired CO_2 can be determined
Mixed expired CO_2 ($PeCO_2$ or $FeCO_2$)	N/A	Yes	Volume-weighted average of CO_2
CO_2 elimination (VCO_2)	N/A	Yes	Net volume of CO_2 measured at the mouth or airway, and calculated as the difference between expired and inspired CO_2
Efficiency	N/A	Yes	Ratio of CO_2 volume contained in the breath and the volume of CO_2 that would have been eliminated by an ideal lung at the same effective volume and end-tidal fractional CO_2
Phase I delineation and duration	Yes[a]	Yes	Time from start of expiration to increase in PCO_2
Volume	N/A	Yes	Volume from start of expiration to increase in PCO_2
Phase II delineation and duration	Yes[a]	Yes	Time: approximate measure available Volumetric: time from end of phase I to intersection of extrapolated slopes of phase II and III
Volume	N/A	Yes	Volume during phase II
Slope	Yes[a]	Yes	Curve fit of central portion of phase II
Phase III delineation and duration	Yes[a]	Yes	Time: approximate measure available Volumetric: Time from end of phase II to end of expiration
Volume	N/A	Yes	Volume during phase III
Slope	Yes[a]	Yes	Curve fit of central portion of phase III
Angles: alpha angle. beta angle	Yes[a]	Yes	Angle between phase II and III and phase III and start of inspiration (for time …ranges between 100 and 110 degrees)
Dead spaces airway (“anatomic”)	N/A	Yes	Volume of the conducting airways at the ‘midpoint’ of the transition from dead space
Physiologic	N/A	Yes	Total dead space includes alveolar, airway and apparatus dead spaces
Alveolar	N/A	Yes	Dead space that is not airway dead space volume and is calculated by subtracting the airway dead space volume from the physiologic dead space
Dead space ratios airway	N/A	Yes	Functional anatomic dead space calculated via Fowler’s method divided by expired tidal volume
Physiologic	N/A	Yes	Total dead space calculated graphically with Enghoff-modified Bohr equation or alternate methods
Alveolar	N/A	Yes	Alveolar dead space volume divided by expired tidal volume

[a] Different context for time and volume

(a) measures from subdivisions of and derivations of the volumetric capnogram, (b) measures from the transformations of the capnogram (e.g. frequency and wavelet transforms), (c) traditional and non-traditional measures of time and volume domain statistical properties (e.g. skew, kurtosis, Hjorth parameters) [38], and (d) measures from transformations of the derived data and features.

- You et al. [23] examined new features based on slopes and area ratios to better characterize the nature of the transition from phase II to phase III in the time capnogram, and related those changes to conventional spirometric measures. Other new parameters have been derived from the volumetric capnogram to provide additional physiologic insight, including efficiency [39] and alveolar ejection volume (analogous to stroke

Table 2 Selected novel features in volumetric and time-based capnography

Feature category	Feature	Comments	References
Indices	Index of Ventilatory Efficiency (IVE)	IVE = VAE/(VT − $V_D$aw)	[132]
		IAH = 1 − [(VT − V_D Bohr)/(VT − V_D aw)]	[132]
	Index of Airways Heterogeneity (IAH)	($PaCO_2$ − $PetCO_2$)/slope phase III	[82]
	PE Index		
Slopes and angles	Take off angle	Angle between baseline and extrapolated phase II slope	[25]
	Residuals	Residuals remaining from linear fit over plateau (phase III)	[25]
	SR1	Ratio of expiratory and alveolar plateau slopes	[23]
	InspSlope	Downward slope at onset on inspiration,	[25]
	ExpSlope	Upward slope at onset of expiration	[25]
CO_2 waveform measures and statistics	MinPlateau	Minimum CO_2 value over plateau	[25]
	Width	CO_2 pulse duration	[25]
	Sharpness	Ratio of mean to standard deviation of CO_2 pulse	[25]
	MinCO_2	Minimum CO_2 value over pulse	[25]
	Skew	Ratio between left and right CO_2 segments	[25]
	Kurtosis	Kurtosis of CO_2 pulse	[25]
	Mean and median	Mean and median values of CO_2 values over expiration	[123]
	STD	Standard deviation of mean CO_2 value over expiration	[123]
	RMS	Root mean square of CO_2 values over expiration	[123]
Frequency transformations	Power spectra	Width and frequency location of fundamental and other components	[63]
	Wavelet		[42]
		Wavelet coefficients	
Hjorth parameters	Activity	Signal power, the variance of a time function	[38]
	Mobility	Proportion of standard deviation of the power spectrum	[38]
	Complexity	Change in frequency—similarity to sinusoidal wave	[38]
Areas	Total_AUC	Cross sectional area under the detectable CO_2 curve	[123]
	AUC3	Area under the alveolar phase	[123]
	Area under curve	Area under time capnogram (expiratory portion) (Not equal to VCO_2exp)	[77]

The features in this table are intended to illustrate the range of features used by the investigators cited in this paper and is not a complete list *VDaw* airway dead space, *VDBohr* physiologic dead space (Bohr method), *CO_2 pulse duration* width of capnogram (see Fig. 2a)

volume) [40]. Romero et al. [40] computed slopes normalized by $P_{ET}CO_2$ (in mm Hg L^{-1}) of two partially overlapping regions of phase III of the volumetric capnogram (50 and 75 % to end tidal PCO_2 point of expired volume) since this is expected to be closer to the spread of ventilation/perfusion ratios.

- The height and width of the peaks from Fourier analysis [41], model parameters determined from autoregressive modeling [41], and coefficients from wavelet analysis [42] have been used as features to classify capnograms.
- The Hjorth parameters of activity, mobility, and complexity—normalized slope descriptors used for extracting features from the electroencephalogram—have been applied by one research group to the capnogram [24].
- Other transformations of the waveform and features, including the natural log [43], have been explored.

The list of potential candidate features is quite large, and only features discussed in the medical literature are referenced in this paper. Bravi et al. [44] provides a thorough list of techniques, including listing the categories of derived features (e.g. statistical, geometric, energetic, time-invariant) in the context of variability analysis that should make it translatable to the analysis of waveforms such as the capnogram.

3 Overview of supervised learning methods

The earliest known applications of classification using features from the capnogram dates to the 1980s and earlier. For those interested, it is suggested that the reader consult accessible introductions to machine learning [e.g. 45, 46] and overviews of techniques potentially useful for clinical application [44].

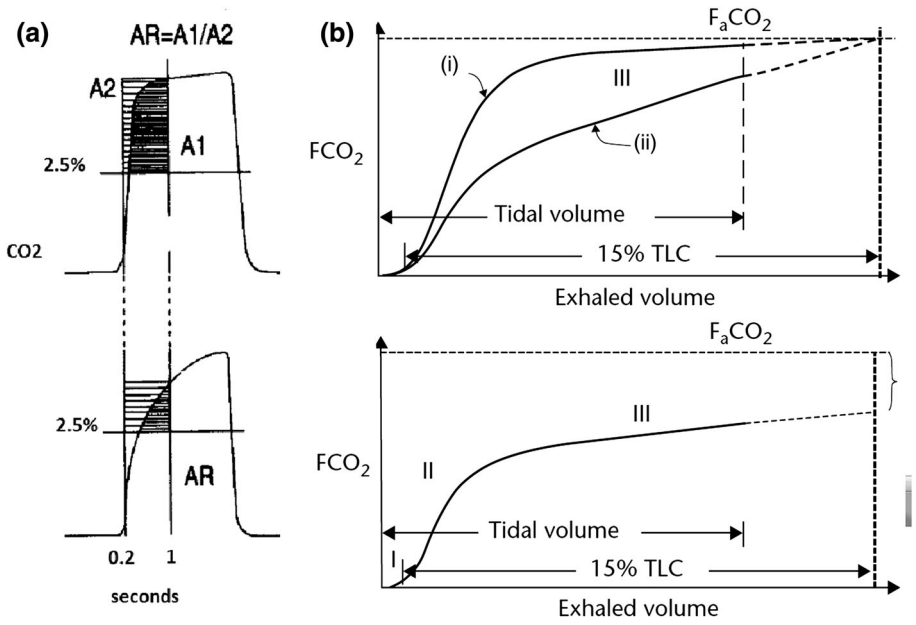

Fig. 3 Novel features from the capnogram including (**a**) area ratio (AR) using the areas bounded as shown describing degree of curvature of the time capnogram (Reproduced with permission of the European Respiratory Society from You et al. [23]), (**b**) differences in the curves and values at 15 % TLC for normal/obstructive disease (*top-i* and *ii* respectively) and pulmonary embolism (*bottom*) used for determining fdlate. (Adapted from Anderson [85]. Reprinted with the permission of Cambridge University Press.)

The approach followed by most of the investigators is to:

1. Define the problem (establish the hypothesis)
2. Acquire a set of waveforms (e.g. capnograms),
3. Preprocess the data and extract features of interest,
4. Partition the data into a training and test data set,
5. Train the classifier(s) or predictor(s) with the training data set while assessing performance with model validation methods (e.g. cross-validation),
6. Evaluate its performance using the test data set, summarizing with various metrics, such as accuracy, correlation (e.g. r, r^2), bias and precision with Bland–Altman plots, and the area under the ROC curve (AUC) and,
7. If possible, prospectively collect additional data for evaluation with the model.

The AUC, a single-number "summary" of classification algorithm performance that is independent of decision thresholds and invariant to a priori class probability distributions [47], will be preferentially presented in this paper if available from the cited studies. The tradeoffs and a very brief description of the different methods employed by the researchers cited in this review are included in Table 3 with the respective references.

4 Clinical applications

The time and volumetric capnographic features that have been used by investigators have been summarized, and aspects of the algorithms used to date for classification, prediction, screening, and detection have been highlighted (Table 4). A number of the studies exploring selected diagnostic and therapeutic applications will be reviewed, with a focus on the features used and the respective learning algorithms applied. This section, divided into classification and prediction, is further subdivided by specific application categories of each, with aspects of screening and detection included within.

4.1 Classification

Classification as discussed in this paper refers to using features derived from the capnogram to classify the candidate capnogram into one of the predefined classes. This may consist of (a) real-time waveform classification/anomaly detection during monitoring (e.g. anesthesia) or (b) classification of a candidate capnogram into one of several disease classes, such as normal, COPD, or CHF. Artifact removal (e.g. cardiogenic oscillations) and/or anomaly identification (e.g. equipment malfunction), although not discussed in detail, is important to both reduce artifact related false alarms and the incidence of recording corrupted data in the patient's electronic health record [48], and serves as a key component of a real-time comprehensive intelligent cardiorespiratory analysis system.

4.1.1 Real-time waveform classification/anomaly detection

The earliest applications of automated real-time methods for classifying capnograms to detect patient and breathing circuit abnormalities were used in anesthesia practice implemented as rule-based expert systems [12, 14, 49, 50],

Table 3 Highlights and tradeoffs of algorithms referenced

Algorithm category	Example algorithms	Problem Type	Results interpretable?	Easy to explain algorithm?	Average predictive accuracy	Performs well with small n?	Irrelevant features handled well?	Learns feature interactions?	References using algorithm
Supervised learning methods									
Regression	Ordinary least squares	R	Yes	Yes	Lower	Yes	No	No	Many, [75]
	Logistic	C	Yes	Somewhat	Lower	Yes	No	No	[68]
Neural networks	Perceptron/back-propagation	E	No	No	Higher	No	Yes	Yes	[32, 41, 51–53, 74, 78]
Decision tree learning	Decision trees	E	Somewhat	Somewhat	Lower	No	No	Yes	[95]
Instance based methods	k-NN	E	Yes	Yes	Lower	No	No	No	[25]
Bayesian	Naive Bayes	C	Somewhat	Somewhat	Lower	Yes	Yes	No	[95] (no results)
Kernel methods	SVM	E	No	No	Higher	Yes	Yes	No	[42, 96]
Discriminant analysis	LDA, QDA	C	Somewhat	No	Lower	Yes	No	No	[66]
Other									
Clustering	k-means	U	Somewhat	Yes	n/a	No	No	No	[51]
Rule based	Expert systems	C	Yes	Yes	Varies	Varies	Varies	Varies	[12–14, 49, 50]

Sources: Table based on material from: http://www.dataschool.io/comparing-supervised-learning-algorithms/ with permission, http://machinelearningmastery.com/a-tour-of-machine-learning-algorithms/ and cited text [46]

k-NN k-Nearest Neighbor, *SVM* support vector machine, *LDA* linear discriminant analysis, *QDA* quadratic discriminant analysis, Problem Type: R- regression, C-classification, E-either, U-unsupervised

Algorithm Category Definitions

Regression models the relationship between the feature variables and the model prediction. With linear regression the dependent variable is continuous whereas with logistic regression the dependent variable is categorical and the output is the probability of the instance being positive

Artificial Neural Networks are a class of pattern matching non-linear models consisting of input, output and hidden nodes where the weighting of each interconnection is determined by a learning process

Decision tree methods construct a tree like model of decisions based on successive partitioning of the feature values

Instance based learning models a decision problem with examples of training data that are considered significant to the model. The k-nearest neighbors (k-NN) algorithm uses as inputs the k closest training examples in feature space and outputs a class (if classification) or average value of the k nearest neighbors (if regression)

Naïve Bayesian methods are probabilistic classifiers which applies Bayes' theorem and assume statistically independent features

Kernel Methods map input features into a higher dimensional features space to perform classification. Support vector machines (SVM) finds the optimal hyperplane that maximizes the distance (i.e. margin) between the output classes

Discriminant Analysis is a classification method that projects high dimensional data to lower dimensions in feature space. With linear discriminant analysis (LDA) a linear combination of features and a linear decision boundary is used. With quadratic discriminant analysis (QDA) a quadratic decision boundary is used

Clustering uses the structures in the feature data to organize the data into groups using usually centroid-based and/or hierarchal approaches

Rule based expert systems—Knowledge often captured as a set of If/Then rules and may use fuzzy logic as well

template matching with rules [13], and artificial neural network classification systems [51–53]. These systems were intended to provide the clinician with actionable information, using the analysis of breath-to-breath waveforms and the presentation of clinically relevant messages (e.g. airway obstruction); and, in some cases, were included as part of a more comprehensive, intelligent, multi-parameter monitoring/alarm system [53, 54, 55], such as using the features of the capnogram with other signals (e.g. flow and pressure) in ANN-based anesthesia alarm systems [55, 56].

Bao [12] constructed a real-time expert system dubbed, the Capnogram Analyzer Expert System (CAES) with development data collected on patients undergoing anesthesia and rules based on the classic *Atlas of Capnography* [16] and the expertise of a local clinician. The CAES analysis used a heuristic rule-based "expert" system, which comprised segmentation with piece-wise linear approximation, breath identification based on these linearized segments, and classification into one of 73 capnographic patterns (e.g. normal, cardiac oscillations, curare cleft). An agreement of 95 % was reported between the manual visual and the automated classification on about 3000 capnograms.

Ventzas [14] developed an "If–Then" rule-based expert system (CAPNEX) intended for both medical diagnostic (e.g. normal, pathological, artifact) and hardware fault detection using time and frequency measures from the capnogram and available pulmonary tests as inputs along with pattern recognition using shape approximations and heuristics. A plot of the preliminary performance of 5 classification rules for a number of situations (e.g. apnea, cardiogenic oscillations) using these measures suggested accuracy as high as 80 %.

Van Genderingen et al. [13], working with Nik (JS) Gravenstein in the anesthesia department at the University of Florida, took a different approach. They had observed many clinicians wonder how to interpret these waveforms. They decided to take on the challenge and implement a classification system, and used this opportunity to display several waveforms side-by-side for comparative purposes. The development capnogram data set, collected on patients undergoing anesthesia, was used with template matching based on a "normal" learned waveform and rules to detect typical/atypical waveforms and certain characteristic waveforms associated with unacceptable ventilator conditions (e.g. airway obstruction and valve malfunction) or physiologic conditions (e.g. patient fighting ventilator). The authors reported successful recognition of spontaneous breathing, circuit disconnection, valve dysfunction and ET obstructions on 28 mechanically ventilated adults over a total of 65 h of testing during general anesthesia.

Navabi [53], as part of his doctoral dissertation on a smart alarm system, developed a two-stage ANN-based classifier using the leading and trailing edges of the capnograms to determine breathing mode (e.g. mechanical or spontaneous) during anesthesia. It was reported that the use of this classifier contributed to a 42 % reduction in low end-tidal-CO_2 false alarms [53].

Goldman [52] applied a PC-based multi-ANN approach to capnograms recorded from mechanically ventilated anesthetized patients to detect patient and breathing circuit abnormalities. The ANN-based system for capnogram analysis includes ANNs for detection of the start and end of a breath, waveform normalization, an ANN for classification into one of seven classes (e.g. normal, spontaneous, inspiratory and expiratory valve defect, patient effort), and an arbitration ANN that considered contextual interpretation and expert input with output of the classification ANN. The classification ANNs were trained with a mechanical lung simulator and tested on patient data collected in the operating room. The arbitration ANN was trained by the outputs of the classifier ANNs, human expert input, and other physiological inputs for the breath (e.g. respiratory rate). A recognition accuracy for normal breaths and breaths with single abnormalities of 96 % was reported.

More recently, Ahmad [57] describes the use of a software tool for capnogram analysis (InCAP-Intelligent Capnography) that includes an embedded clustering (k-Means) algorithm to assign classes and additional routines for identifying end-tidal CO_2 and waveform features (e.g. angles). To evaluate performance, the InCAP-derived parameter estimate from spontaneously breathing patients was compared to monitor-displayed end-tidal PCO_2 values. For those with the availability of $PaCO_2$ reference values, InCAP estimates were deemed more accurate.

Bleil [51, 58] implemented on a mobile device two algorithms, a simple cluster-by-correlation using resampled and amplitude-normalized same-time length capnograms, and a ANN algorithm to classify these resampled capnograms into one of four ventilatory categories (controlled ventilation intubated, spontaneous breathing intubated, spontaneous breathing extubated, sleepy). The reported classification category accuracy, typically greater than 66 %, varied as a function of ventilation category.

Real-time waveform-based classification and anomaly detection systems that utilize features from the capnogram have demonstrated high levels of performance, but have yet to see widespread clinical application. With increased interest in paradigms, such as remote monitoring, it is expected that the approaches reviewed will find greater acceptance and use in clinical practice.

Table 4 Summary of selected investigators work using the capnogram for classification, and prediction

Lead author affiliation/ location	Pub. Year	Purpose	Approach	Groupings (training:test sets)	Selected features—Capnogram[a]	Performance[b] (Accuracy %/ AUC (0.xx))	References
Real-time waveform classification/anomaly detection							
W. Bao (MS), Vanderbilt Univ.	1987	Monitoring	3 stage Expert System	n/a	$P_{ET}CO_2$, rate, shape descriptors	95 % with visual class	[12]
Van Genderingen, Gainesville, FL	1987	Monitoring	Template matching and rules	n/a	Waveform, and times of phases	n/a	[13]
Navabi (PhD), U Arizona	1990	Monitoring	Two-stage ANNs (breath type)	(5:12)	Samples in time window of capnogram	85 % mech breaths	[53]
Goldman, Denver, CO	1991	Monitoring	ANNs—start/end breath, classification	(Simulator:OR data)	Input- one complete capnogram cycle	96 %	[52]
Ventzas, Athens, Greece	1994	Monitoring	Expert systems with FFT and pattern matching	n/a	Frequency content, plateau level, timing	n/a	[14]
Smith, England	1994	Cardiogenic oscillations	Rules	1698 breaths	$P_{ET}CO_2$, insp/exp times & min. inspired	99.2 %	[50]
Rader, Pomona, CA	1994	Monitoring	Rules based expert system	n/a	14 features database	n/a	[49]
Bleil (MS), U Lubeck	2008	Monitoring	Cluster by correlation/ANN	32 patients (2/3:1/3)	Resampled capnogram (all)	varies	[51] [58]
Classification of a candidate capnogram into one of several disease classes (with one of the classes normal)							
You, France	1994	Asthma	Correlation of features with spirometry	n/a	Slope, areas, ratios, angles	Sign. Corr. with spiro. features	[23]
Yaron/Druck Y/D, Colorado, USA	1996 2007	Asthma	Correlation of features with PEFR	Y: 20+/28−D: 13 adults	Y: Slope PIII D: VCAP slope PIII	Y: r = 0.84, $p < .001$ D: r = 0.7, $p < 0.2$	[62] [61]
Kean, Malaysia	2010	Asthma	ROC analysis	34 patients 16+/ 18−	You [23] and Hjorth params (activity)	SR 0.92 Activity 0.90	[24]
Kazemi (PhD), Malaysia	2012	Asthma	ANN (1–5 to asthma severity)	73+/23−	LPC coefficients and PSD freq components	DR/ER 90.15/9.85 %,	[63]
Pomares, Cuba	2014	Asthma severity	Support vector machine	22 asthmatics	Wavelet coefficients	sens/specif. 100/91.43 %	[42]
Mielosyzk (MS), MIT, Cambridge, MA	2014	COPD/CHF/ Normal	quadratic discriminant analysis (QDA)	N, CHF, COPD (20,31,33: 10,22, 23)	breath duration, peak $P_{ET}CO_2$, exp slope, time at peak $P_{ET}CO_2$	0.89 COPD/CHF 0.98 normal/ COPD	[66]
Estimation of the value of an inaccessible or invasively determined physiologic parameter							
Rayburn, Washington, DC	1997	Estimate $PaCO_2$	ANN	23 patients	VCAP slopes, indices, intercept, angles	Claims ± 2 mm Hg of $PaCO_2$	[74]
Chuang, Taiwan	2012	Estimate $PaCO_2$	Linear regression	41 patients	$P_{ET}CO_2$, DLCO, VT, SVC, MEP	AIC 1.099	[75]
Prediction for the presence or absence of disease condition							
Kline (Patel etc.), S Carolina	1999	Pulmonary embolism	Linear regression ANN (Patel)	Several studies	Area, VDalv/VT, D-dimer, VCAP params	P- sens/spec 100/48 %	[77–80]
Verschuren, Brussels, Belgium	2010	Pulmonary embolism	ROC analysis	239 patients w capno.	VDalv/VT, PE index, fdlate	All VCAP corr. degree obstruct	[82]

Table 4 continued

Lead author affiliation/ location	Pub. Year	Purpose	Approach	Groupings (training:test sets)	Selected features—Capnogram[a]	Performance[b] (Accuracy %/ AUC (0.xx))	References
Guide the administration of therapy (in OHCA)							
Krizmaric, Slovenia	2009	Outcome of CPR	Decision trees (and other methods)	477 adults	Arrival time, witness, bystand. CPR, $P_{ET}CO_2$	87 % accuracy	[95]
Shandilya (PhD), VCU, Virginia	2012	Defib success	Support vector machine	57 adults	Time/wavelet features ECG & CO_2	AUC/accuracy 0.94 83.3 %	[96]
Prediction of the future morbidity or mortality of a patient with a condition							
Hubble, Durham, NC	2000	Extubation predictor	Logistic regression	45 children	VD/VT phys,	$p < 0.0001$	[69]
Nuckton, San Francisco, CA	2002	Predict Risk of dying	Logistic regression	179 ARDS patients	VD/VT phys (and other clinical parameters)	VD/VT phys $p < 0.001$	[68]
Kartal, Turkey	2011	Metabolic disturbance	Logistic regression (low bicarbonate)	240 adults	$PetCO_2$	AUC 0.734	[101]
Rasera, Brazil	2015	Extubation	ROC analysis	82 infants	SR, alpha angle, $PaCO_2$	AUCs $\sim$ 0.92	[100]

MS for Masters, PhD for doctorate, *AIC* akaike information criterion, *ANN* artificial neural network, *AUC* area under ROC curve, *FFT* fast Fourier transform, *LPC* linear predictive coding, *OHCA* out of hospital cardiac arrest, *PEFR* peak expiratory flow rate, *PSD* power spectral density, *VCAP* volumetric capnogram, *insp* inspiratory, *exp* expiratory, *Defib* defibrillation, *mech* mechanical, *DR/ER* detection rate/error rate, ± = with/without disease

[a] See Tables 1 and 2 for parameter definitions

[b] Accuracy or AUC shown unless otherwise noted

4.1.2 *Classification of a candidate capnogram into one of several disease classes*

The differences in the shape of the capnogram between normal subjects and those with obstructive (e.g. asthma, COPD) and restrictive lung diseases have been known since the 1960s. Investigators have explored the viability of using a number of different features to quantify those differences in both time and volumetric capnograms (e.g. [59, 60]) and correlate with spirometric measurements [23]. These differences are often apparent in the tracings of subjects with these obstructive and restrictive lung diseases (e.g. asthma, COPD, CHF) (Fig. 4). The leading end of the expiratory portion of the time capnograms from subjects with obstructive disease rises slower than in normal subjects with a shape described as a shark's fin and significantly different frequency content than a normal capnogram (Fig. 5). The features researched have included the slope of the alveolar plateau, the radius of the minimal curvature of the angle Q (i.e. approx. the alpha angle), the time required for the capnogram to transition from 25 to 75 % of the end-tidal PCO_2 value, and the angle formed by the intersection of the lines fitting to the alveolar plateau and central portion of phase II (i.e. alpha angle) [23] The literature describing changes in the capnogram due to restrictive diseases, such as congestive heart failure and the associated lung edema, is relatively limited.

With respect to asthma, researchers have explored utilizing shape measures of the time capnogram [23] and volumetric capnogram [61] to:

a. classify subjects as normal or asthmatic;
b. estimate asthma severity; and,
c. serve as a surrogate measurement for effort-dependent pulmonary function tests, such as peak expiratory flow rate (PEFR) [61].

You et al. [23] assessed the reproducibility of the capnogram and its correlation with standard measures of airway obstruction using computed features from the time capnogram in healthy and asthmatic patients including various slopes, areas, and ratios of slopes and areas. In 10 control subjects and 30 asthmatic subjects, all of the computed capnographic indices were found to strongly correlate with the spirometric parameters of $FEV1_{\%\ pred}$, PEFR and FEV_{25-75}) ($p < 0.001$).

Yaron et al. [62] performed a small prospective study in adults in the emergency department of a hospital (20 asthmatics, 28 normals) to assess whether the slope of the alveolar plateau (i.e. slope of phase III or dCO_2/dt) from the time capnogram can serve as an effort-independent non-invasive measure of bronchospasm. Values for PEFR, the standard approach for assessing airway obstruction in this patient population, and dCO_2/dt were measured for each subject and for the asthmatic both pre- and post-bronchodilator administration. They concluded that $dCO_2/$

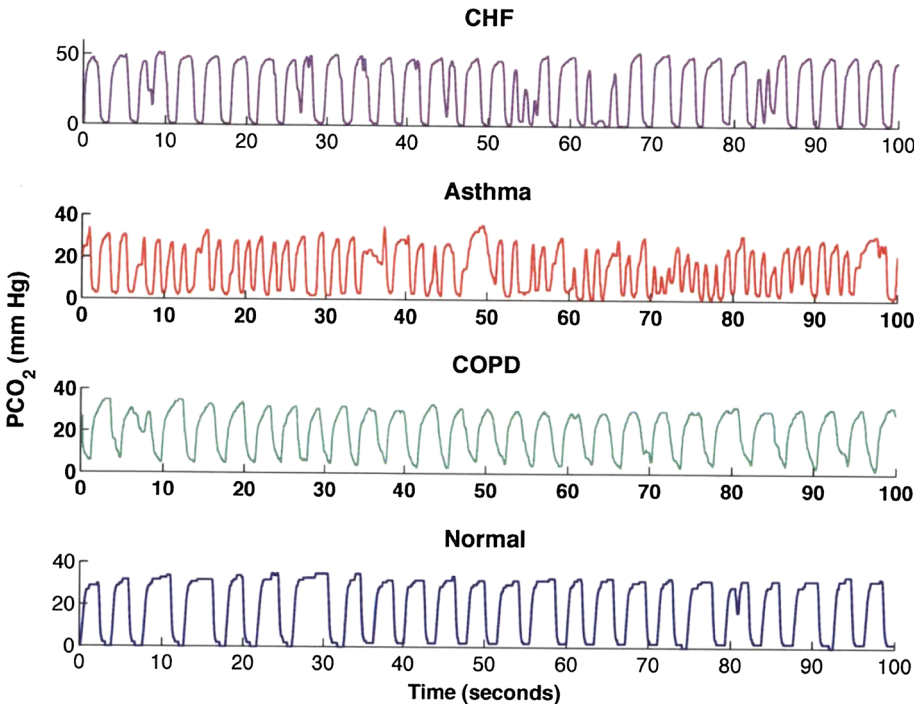

Fig. 4 Representative tracings of the time capnogram from CHF, asthma, COPD and normal subjects (Reprinted from Asher R. Capnographic analysis for disease classification [Masters of Science]. Massachusetts Institute of Technology; 2010 with permission from Massachusetts Institute of Technology) (Also see Mieloszyk [66])

dt (a) serves as an effort-independent measure of bronchospasm in patients with asthma and (b) correlates with PEFR (dCO_2/dt to log(PEFR) $r = 0.84$, $p < 0.001$), Druck et al. [61], working with Yaron, looked to extend their prior work of effort-independent surrogates by examining the relationship between the change in PEFR and change in the slope of phase III from the volumetric capnogram for measurements recorded pre- and post-bronchodilator therapy. The percent changes between PEFR and its surrogate were found be correlated ($r = 0.7$, $p < 0.2$, $n = 13$).

Kean et al. [24] studied the classification performance of novel statistical features computed from the capnograms of 18 non-asthmatic and 16 asthmatic emergency room subjects. The features extracted included those defined by You [23] and included the Hjorth parameters of activity, mobility, and complexity [38] computed over the complete breath cycle, and from the time 4 mm Hg is reached in phase II to the time of the end-tidal maximum value. They found that when the slope ratio (i.e. phase III slope/phase II slope) of the capnogram and the Hjorth parameter activity was computed over a complete cycle, AUCs of 0.9167 ($p < 0.0001$) and 0.8958 ($p < 0.0001$) were produced, respectively, the highest two values of those tested.

Kazemi [41, 63] collected 23 non-asthmatic and 73 asthmatic capnogram data sets from emergency department patients with breathing complaints using a nasal cannula connected to a sidestream capnometer. Significant inter-breath variability of the first order statistics such as the mean and variance was found, as might be expected, leading the author to characterize the capnogram as nonstationary—that is, the statistical properties of the signal changes over time. From the capnogram, features were extracted using different ways of representing non-stationary signals in both the time domain, with linear predictive coding (LPC), and the frequency domain, with an autoregressive model for representing the power spectral density (PSD). From extracted features, five features (all with individual AUCs > 0.7) were selected for classification, including 2 LPC coefficients, and, from the PSD, the first component frequency and magnitude and total number of frequency components were selected. Using the five features from the asthmatic and non-asthmatic capnograms, classification with a ANN, with an integer output directly related to asthma severity, reported detection and error rates of 90.15 and 9.85 %, respectively.

Pomares [42] describes a method for assessing asthma severity using feature extraction from the capnogram based on wavelet decomposition [64]. The features were determined by the decomposition of waveform segments (e.g. upslope, plateau and downslope) of the time capnogram using high and low pass filtering of each segment, downsampling, and determination of the Haar wavelet coefficients (i.e. sequence of rescaled "square-shaped" functions), with multi-resolution analysis by segments based on wavelet transformation. Using a support vector machine (SVM) classifier with a Gaussian Radial Basis function kernel, the input coefficients for each capnogram were classified into one of six severity classes. The highest performing feature vector comprised segments consisting of the leading and trailing edges of the time capnogram

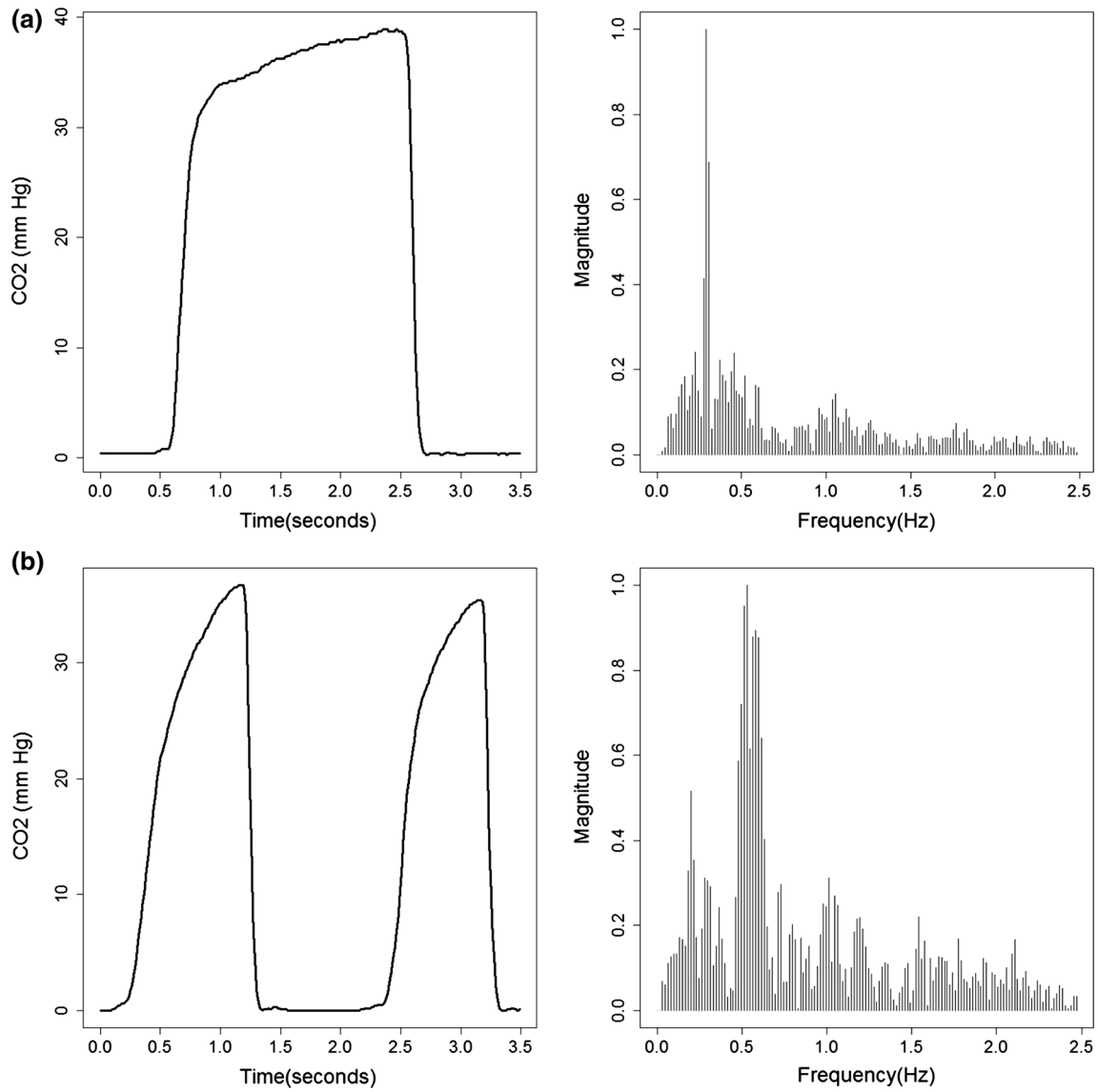

Fig. 5 Selected **a** normal and **b** obstructive disease time capnograms from mechanically ventilated patients on pressure support ventilation with frequency spectrum (Normalized Magnitude) shown (analyzed 1 min of 100 Hz waveform data, Hanning windowed prior to FFT, plots and data analysis using R Studio) Note: largest peak at respiratory rates of approx. 15 and 30 breaths/min; spectral difference due in part to slower rise of obstructive waveforms. (Waveform data courtesy of Convergent Engineering, Gainesville, FL)

with a sensitivity and specificity of 100 and 91.43 %, respectively using the full dataset for testing thereby biasing the reported results.

The studies described so far in this section have sought to differentiate normal from asthmatic patients, assess asthma severity or assess the viability of a surrogate measurement for a forced maneuver. Investigators using features from the capnogram, have also sought as well to differentiate capnograms from normal subjects and those with obstructive (i.e. asthma and COPD), and restrictive diseases.

In a prospective observational study of 49 emergency department (ED) adult patients with moderate-to-severe dyspnea, Brown [65] concluded that no single level of end-tidal PCO_2 could reliably differentiate between cardiac and obstructive causes of respiratory distress ($p = 0.038$). The study also examined the differences between the two groups using demographic (e.g. age) and other clinical parameters, including the presence of certain lung sounds, and found significant differences between the groups for a number of these parameters, suggesting that a model, including context and some of these parameters, should have a greater ability to differentiate the two groups.

Mielosyzk [66] used a quadratic discriminant analysis (QDA) with bootstrapping to differentiate between time-

based capnograms in spontaneously breathing subjects classified as normal, chronic obstructive pulmonary disease (COPD), and congestive heart failure (CHF). The capnograms, obtained using a nasal cannula connected to a sidestream gas analyzer, were collected from several institutions, and included 30 normal subjects, 56 COPD patients, and 53 CHF patients. After preprocessing, features from each breath were computed for the first 80 valid preprocessed exhalations for each subject including the exhalation duration, maximum PCO_2 value during exhalation (i.e. typically the $P_{ET}CO_2$), time spent at the $P_{ET}CO_2$ value within a window of ±0.5 mm Hg, and the end-exhalation slope (linear regression of last 5 PCO_2 values representing the last 100 ms). Using an ensemble approach, with 50 random partitions of data for each patient grouping (i.e. normal, CHF, COPD) for the training data, multiple base classifiers (i.e. QDA boundaries) determined, using a voting rule, the overall classifier. The training of the classifier, consisting of 20 normal, 31 CHF, and 33 COPD patients, employed a 10-fold cross-validation approach. For each fold, 50 datasets, each created from a random 70 % of the subject records were classified with QDA, with the remaining 30 % used for tuning. A test set (10 normal, 22 CHF, 23 COPD), using an ensemble approach with the training set overall classifier, determined the final classification for each test record. This approach was applied to differentiate COPD from CHF and COPD against normal records using an approach based on individual breaths and one based on the mean value of each of the features for each subject record. With the test set, AUCs of 0.89 (95 % CI 0.72–0.96) and 0.98 (95 % CI 0.82–1.0) were reported for the COPD/CHF and COPD/normal classifications, respectively.

Research remains active and promising with respect to classifying patients for the presence or degree of obstructive and restrictive lung disease based on features from the time and volumetric capnogram, with a positive outlook for possible inclusion in medical devices, middleware, or mobile platforms, and integration into screening protocols and treatment algorithms.

5 Prediction

Features from time and volumetric capnograms, often in combination with other measures, have been utilized to (a) estimate the value of an inaccessible or invasively determined physiologic parameter, (b) screen for the presence or absence of a disease condition, (c) guide the administration of therapy, or (d) predict the prospective morbidity or mortality of a patient with a presenting condition. These clinical applications will be reviewed with relevant examples.

Estimating inaccessible parameters, such as alveolar PCO_2, or invasively determined parameters, such as arterial PCO_2 by using features from the time or volumetric capnogram has been undertaken by several groups over the last two decades. The ability to estimate these parameters has allowed the noninvasive calculation of physiologic and alveolar-to-tidal volume dead space and the associated ratios. Investigators have explored screening, primarily in the emergency department setting, for the presence or absence of pulmonary embolism (PE) to assess the need for confirmatory imaging and the administration of thrombolytic agents. While end-tidal PCO_2 changes have been reported to be sufficient justification in the case of massive PE, features from the volumetric capnogram, such as alveolar or physiologic dead space ratio - alone and in conjunction with blood tests (D-dimer)—have and continue to be evaluated as screening tools. With the relationship of end-tidal CO_2 to cardiac output in low flow states (e.g. cardiac arrest) established, the role of end-tidal PCO_2 as a predictor of survival and its use as real-time feedback on the effectiveness of compressions is an ongoing topic of research. [67] Investigators have used features from the capnogram to assess the likely morbidity or mortality of a patient with a condition such as ARDS [68] and predict successful extubation [69].

5.1 Estimation of the value of an inaccessible or invasively determined physiologic parameter: arterial and alveolar PCO_2

The benefits of managing arterial carbon dioxide, directly or via surrogates, include the maintenance of cardiac output, tissue oxygenation, perfusion, intracranial pressure, and cerebrovascular reactivity [70]. With the current technology, the estimate of arterial PCO_2 requires blood sampling and its analysis. On the other hand, alveolar dead space and PCO_2 are physiologic concepts and determined indirectly. Surrogates and methods for assessing arterial and alveolar PCO_2 continue to be explored, including end-tidal PCO_2. A large number of studies over the past few decades investigating the viability of using end-tidal CO_2 as a surrogate for arterial CO_2 in different patient groups have reported a wide range of conclusions, with some even questioning the value of capnography in the tested clinical environment. In general, these studies have not considered patient differences in physiologic dead space and the interrelated gradient between end-tidal and arterial PCO_2 [20] The physiologic (e.g. dead space and shunt, stability of carbon dioxide stores in the blood and lung [71]), technical (e.g. choice of measurement technology, patient interface and positioning), and other complexities (e.g. types of patients studied and their stability) complicate the comparison of arterial values to end-tidal PCO_2 values, and cloud how accurately and reliably measurements from the breath can reflect arterial or alveolar measurements.

Banner [72] and McSwain [20] studied mechanically ventilated adults and children, respectively, and reported a similar and significant statistical correlation between $P_{ET}CO_2$ and $PaCO_2$, which decreased with increases in the physiologic dead space ratio ($V_D/V_{T\ phys}$) (Table 5) and showed predictable increases in the arterial-end-tidal gradient with increases in $V_D/V_{T\ phys}$. [20] Although the majority of the published studies have involved simple correlation studies, other approaches for predicting arterial PCO_2, have included genetic algorithms [73], artificial neural networks [74], and linear regression [75].

Chuang et al. [75] is included in this review, as this study represents the application of both univariate and multivariate models to predict arterial PCO_2 in COPD patients during a maximal exercise test on a cycle ergometer. They conducted a brute force study evaluating with regression all available data subsets, including demographic, anthropological, and noninvasive clinical measurements. They reported that, individually, $P_{ET}CO_2$ and $FECO_2$ showed the lowest Akaike information criterion (AIC) values, respectively, and with multivariate analysis, the best prediction equation for $PaCO_2$, was found to be a function of $P_{ET}CO_2$, slow vital capacity, maximum expiratory pressure, diffusing capacity for carbon monoxide, and tidal volume.

Research and clinical interest in reliable and validated noninvasive surrogates for arterial and alveolar PCO_2 for use in the management of patients for a range of clinical applications and environments remains. Improved analysis methods and physiologic models, and the integration of these models to enhance understanding can help increase confidence in the use of these measures.

5.2 Prediction for the presence or absence of disease condition: PE screening

Accurately distinguishing patients with a pulmonary embolism (PE+) from patients without a pulmonary embolism (PE−) on clinical presentation in the emergency department remains a challenge. With the pre-test probability of a PE in the general emergency room population being low, testing is performed erring on the side of false positives. It is known that PE-associated ventilation/perfusion (V/Q) mismatch, and the related increase in the physiologic dead space, is an indication of significant PE by the quantitative changes of the end-tidal PCO_2 value over time [76] as well as in the general features of the capnogram. As such, features from the time and volumetric capnogram, alone and in conjunction with other measurements such as the D-dimer assay, have been considered for use in diagnostic algorithms to maximize the sensitivity of this screening test prior to performing further confirmatory tests such as the spiral CT or perfusion scan. Features of capnogram studied have included area under the time capnogram [77], CO_2 (e.g. end-tidal PCO_2), features (e.g. flow, time and slope) from the volumetric capnogram [78], alveolar dead space ratio [79], alveolar space ratio and D-dimer [80], late dead space fraction (fdlate) [81], PE index [82], D-dimer and $PetCO_2$ [83], and D-dimer and exhaled CO_2 and O_2 for segmental PE [84].

An early application of artificial neural networks (ANN) for determining the presence of a pulmonary embolism (PE), Patel [78] used features from a volumetric capnogram collected from subjects breathing spontaneously through a mouthpiece interfaced to mainstream CO_2 and flow sensors. A test set of 12 subjects (6 PE+ and 6 PE−), with 17 variables from a volumetric capnogram served to train a full connected back-propagating ANN, with an output between 0 and 1 with 0 representing no PE and 1 PE (0.2–0.8 considered undecided). Pulmonary embolism was confirmed by lung scan or pulmonary angiogram. Of the 17 variables examined (Table 4 in [78]), the six variables found to be significantly different between the groups were end-tidal PCO_2, slope of phase III, peak expiratory flow, spontaneous and alveolar ventilation, and inspiratory time. The derived model, evaluated with a test set of 53 subjects (30 PE+ and 23 PE−), reported a sensitivity and specificity of 100 and 48 %, respectively.

Of particular interest, the derived parameter, $f_d$late [81]—ratio of the difference between the arterial PCO_2 and a PCO_2 value determined by extrapolating the phase III line to a volume at about 15 % total lung capacity and arterial PCO_2 (Fig. 3)—was reported to more effectively detect PE than other capnographic variables with AUCs from various studies for $f_d$late, V_{Dphys}, V_{Dalv}, Pa-etCO_2, and $P_{ET}CO_2$ of 0.96, 0.73, 0.84, 0.86 and 0.83, respectively [85].

Despite the common sense physiologic basis for the use of dead space ratios and related measures in the diagnostic screening algorithm for PE, clinical studies to date have yet to demonstrate a level of evidence significant enough to permit inclusion in practice guidelines [86]. A recent meta-analysis [87] of 14 trials with 2291 total subjects and a

Table 5 Relationship of $P_{ET}CO_2$ and $PaCO_2$ with physiologic dead space

Children[a]			Adults[b]	
$P_{ET}CO_2$ and $PaCO_2$			$P_{ET}CO_2$ and $PaCO_2$	
VD/VT	r^2	Mean gradient (mm Hg)	V_D/V_T	r^2
≤0.4	0.90	0.3 ± 2.1	<0.60	0.91
0.41–0.55	0.77	5.9 ± 4.3		
0.55–0.7	0.74	13.6 ± 5.2	>0.60	0.54
>0.7	0.56	17.8 ± 6.7		

Data excerpted from: [a] McSwain [20] (56 mechanically ventilated pediatric patients), [b] Banner [71] (31 intubated adults)

20 % overall prevalence of pulmonary embolism reported pooled values for sensitivity and specificity of 0.80 and 0.49, respectively (AUC 0.84), and concluded a possible role for capnography when PE pretest probability is 10 % or less. Improvements in the computational methods of curve fitting the volumetric capnogram and noninvasively estimating alveolar PCO_2 and dead space in combination with advanced predictive algorithms may offer additional life to this approach.

5.3 Guide the administration of therapy

Therapeutic interventions with features from the time or volumetric capnogram can serve an important role and dates back to the use of estimated alveolar carbon dioxide levels for the management of iron lung-dependent polio patients [88]. The role of these features for the management of ventilation (invasive and noninvasive), including optimal PEEP, weaning and delivery of gas therapies are not discussed in depth other than the role of capnography during CPR as follows.

5.4 CPR survival and guide to effectiveness of compressions

The potential value of features of the capnogram, such as utilizing end-tidal PCO_2 as a guide to resuscitation, has been known for several decades [89], with different end-tidal PCO_2 cut-off values (e.g. 10 mm Hg) analyzed as predictors of death after an extended period of life support without a pulse (e.g. 20 min) [21]. A recent case report [90] highlights the value of capnography during a prolonged period of cardiac arrest (96 min) in which resuscitation was continued solely on the basis of end-tidal PCO_2 values at or near normal, resulting in a complete neurologic recovery by the patient. A systematic review of the prognostic value of end-tidal PCO_2 during cardiac arrest [91] supports the view that end-tidal PCO_2 values during CPR does correlate with the likelihood of the return of spontaneous circulation (ROSC) and survival; however, the use of specific end-tidal PCO_2 cut-off values during CPR to accurately predict the outcome of resuscitation remains to be determined. In low cardiac output states, as during cardiac arrest, it has been demonstrated that end-tidal PCO_2 values tend to be more dependent on compression-driven cardiac output and less dependent on CO_2 production and ventilation. This has led to the exploration of other capnographic features to predict ROSC (e.g. area under curve, slopes, cumulative max end-tidal PCO_2) [92] and the suggestion by researchers [67] and companies [93, 94] to use the features of the capnogram (e.g. end-tidal PCO_2, VCO_2) as inputs to algorithms for assessing the efficacy of and controlling chest compressions.

In one study of particular interest, Krizmaric [95] explored the application of several supervised learning techniques, including decision trees, to predict the outcomes of 477 adults with out-of-hospital cardiac arrest using end-tidal PCO_2 values and situational and contextual data (e.g. witnessed cardiac arrest). The authors noted that although the classification accuracy of decision trees was generally not as high as other learning techniques for the subset analysis, the decision trees, considered more interpretable, were reported to perform better as a whole on the dataset (87 % accuracy). This method also recorded arrival time, witnessed arrest (yes/no), bystander CPR (yes/no), and end-tidal PCO_2 (both initial and final values) as significant predictors of outcome.

Shandilya [96] applied non-linear signal processing and learning algorithms to a dataset representing 57 out-of-hospital cardiac arrests (OHCA) in order to predict defibrillation success based on the analysis of ventricular fibrillation waveform with and without features from the time capnogram. Using time domain and complex wavelet-derived features (e.g. energy, entropy) extracted from both the ECG and capnogram and selected by a feature-ranking algorithm, a support vector machine model, chosen given the limited size of the training data set, was used for classification. Evaluation of the models (with 6–10 features) indicated that the inclusion of the capnogram features increased the AUC and classification accuracy from 85 to 93.8 and 82.2–83.3 %, respectively, with the expectation of further improvements with larger training sets.

With the advances in prediction and titration algorithms, heightened focus on prehospital care, additional clinical evidence of the positive correlation of increased compression rate and depth with end-tidal PCO_2 [97, 98] and the introduction of automated CPR devices (e.g. ZOLL® AutoPulse®, Zoll Medical, Chelmsford, MA; LUCAS™ CPR, Physio-Control Inc. Lund, Sweden), the inclusion of capnographic parameters reflecting ventilation and cardiac output in the diagnostic and treatment algorithms for CPR may not be far off.

5.5 Prediction of the future morbidity or mortality of a patient with a condition

Features from the capnogram have been evaluated as tools for decision-making, such as predictors of disease outcome (e.g. ARDS), procedural outcome (e.g. extubation), and exclusion of conditions. Due to the known increase in pulmonary dead space associated with ARDS, a research group at UCSF evaluated its use as a predictor of hospital mortality [68]. Researchers have evaluated end-tidal PCO_2 as a predictor of outcome and status of dead space to predict successful extubation in children [69] and adults [99] as well as simpler features such as end-tidal and

arterial PCO_2 [100]. End-tidal PCO_2 as a widely available parameter continues to find use in new applications, and has been investigated as a possible tool to non-invasively assess metabolic status (i.e. of low bicarbonate) [101].

Nuckton et al. [68] evaluated physiologic dead space ratio measured early (within 10.9 ± 7.4 h) in the development of ARDS, as well as a number of other variables and used logistic regression to assess their possible association with a higher risk of dying, prior to discharge in 179 intubated patients. Several parameters (e.g. PaO2:FiO_2, pH, respiratory compliance) and scores (lung injury score, oxygen index, SAPS II score), as well as dead space fraction and weight-normalized dead space (ml/kg) showed a significant difference between the survivor and non-survivor groups ($p < 0.001$).

Hubble [69], using logistic regression, found that of the 20 pre-exubation demographic and clinical parameters evaluated in 45 mechanically ventilated children, only the mean values of $V_D/V_{T\ phys}$ pre-extubation between the successful and unsuccessful groups were highly significant ($p = 0.0001$), with PaO_2 being the only other variable showing significance ($p < 0.05$). A. It was also found that of the 25 patients with $V_D/V_T < 0.50$, 96 % (24/25) were successfully extubated while only 20 % (2/10) of the patients with $V_D/V_T > 0.65$ were successfully extubated with the intermediate range (0.51–0.65) less predictive.

Rasera et al. [100], in an observational study of 82 intubated infants, concluded that, individually, the mean values of end-tidal and arterial PCO_2 and six of 10 previously studied features could effectively separate the extubation success and failure groups. The features with AUC reported greater than 0.90 included slope ratio, alpha angle, and arterial PCO_2, with AUCs of 0.923, 0.919 and 0.924, respectively, with end-tidal PCO_2 just short of this value with an AUC of 0.895.

Given the healthcare system's pressure to provide a higher quality of care at a lower cost is driving research to develop measures that will help optimize the delivery of care to the patient population as a whole and provide guidance in clarifying whether interventions will likely have an impact on an individual patient morbidity or mortality.

6 Discussion

This paper has sought to highlight and summarize the features derived from the time and volumetric capnogram, the broad array of learning algorithms that can be applied to it, and the breath of clinical applications of these features and their role in various therapeutic interventions. The division of clinical applications and the respective studies between classification and prediction in this paper, although may be of debate, is intended to highlight these applications and the opportunities that remain to be pursued. A significant number of these applications of time and volumetric capnography, including some that have been discussed herein, are highlighted in a chapter in a recently published text on monitoring [6], along with their status as accepted, in development, or speculative. For additional detail on these applications, the reader is advised to consult a review or text on the topics [102].

The performance of the algorithms highlighted in this paper hinge on the fidelity of the data analyzed and how well it reflects the underlying disease states. The choice of measurement technology, patient interface and its positioning influences the fidelity of the measurement. The required bandwidth and data sample rate necessary is dependent on technical aspects of the capnograph and physiological aspects of the patients, with mainstream measurements providing greater fidelity. The minimum sampling rate and data collection system bandwidth will vary as a function of the spectral content of the waveform, with higher sampling rates needed for smaller tidal volumes and higher respiratory rates. It is important that the effect of technology be understood given the limiting factors of design choices, such as side stream vs mainstream measurement, sample cell configuration, detector response time, and signal to noise ratio. Additional tools to assist the testing and development of these smarter systems are needed, including metrics for quality assessment, dynamic physiologic models to permit easier interpretation, consensus standards for devices that provide for external querying of the device capabilities, and simulators for robustly testing the front end and complete signal path.

Herry [25] notes that, to advance the field of respiratory waveform analysis, a need exists for algorithms that assess the capnogram signal quality; and discusses the use of a composite quality index for respiratory analysis (e.g. variability analysis) based on a combination of metrics, such as the percentage of time breaths within physiological limits, classified as normal, and consecutive normal breaths present. To determine the quality of a breath, they performed segmentation, feature extraction, and classification of time capnograms into normal or abnormal classes. They evaluated the performance of decision trees, K-nearest neighbor (KNN) and Naïve Bayes (NB) classifiers, using an initial 15 characteristics extracted from the time capnogram and a reference set of waveforms that were visually annotated. Of interest, the feature selection resulted in three features in common for the three algorithms—residuals after linear fit over plateau, width of CO_2 waveform, and minimum CO_2 over the width. Evaluation with the test set for the three classification algorithms resulted in AUCs of 0.90, 0.88 and 0.89 reported for DT, NB and KNN, respectively.

The use of physiologic models (e.g. compartmental) in automatically interpreting the capnogram has been limited to research. The opportunities to use these models to help make a difference in clinical care are becoming increasingly apparent. Off-line modeling of the respiratory system using compartmental models and the "capnigram", with an expression containing two exponential functions [110], has been in use since the 1960s. Buijs et al. [111] reported using a recursive Bayesian filtering approach to reliably track parameters in real-time with simulated waveforms, which permitted the prediction of unobservable parameters, such as alveolar CO_2 tension, and enabled earlier alerts to changes in the respiratory status. Such models that can adapt, predict and display on a real-time basis "physiologically meaningful" parameters are an area of current commercially funded research [112]. The model parameters (e.g. cardiac output, V_D/V_T phys) should explicitly include both measurable and observable parameters as well those not directly observable with time and volumetric capnography. These models should include context (e.g. location and EMR data) and be embedded in an interoperable monitoring or therapeutic platform. The models can assist the clinician at the point of care to (a) perceive the current state of the patient, (b) simulate consequences to the patient that would result from alternative interventions, and (c) obtain insight that supports bedside clinical decision making.

Updates to relevant device standards (e.g. ISO 80601-2-55: 2011), availability of waveform databases [113], and improved test methods, including gas waveform simulators [114] that can accurately play back pre-recorded carbon dioxide waveforms, should allow for improved device and derived model performance and greater interoperability, as well as provide a means to more effectively and robustly evaluate and compare systems.

With respect to volumetric capnography, a consensus review by 16 of the leading European intensivists noted the important potential of volumetric capnography, as in the management of ARDS; however, its widespread use was limited by complex analysis [115]. This has led to some investigators exploring alternatives to measuring V_D/V_T such as simpler 'user-friendly' indices including prediction equations for V_D/V_T and new ratios to track changes in ventilatory efficiency [116]. Sipmann et al. [117] note that advances in gas measurement technologies and algorithms have led to improvements in the reliability and clinical utility of volumetric capnography and revival of earlier paradigms, such as the breath-to-breath calculation of dead space using an estimate of alveolar PCO_2, as from the mid-portion of phase III of the volumetric capnogram [118]. It is also worth noting that although not yet called out specifically, the ASA Basic Monitoring standards, in addition to requiring the monitoring of carbon dioxide, strongly encourages monitoring the other component of volumetric capnography, that is, exhaled volume. With greater integration and improvements in flow and CO_2 technologies, it is likely that volumetric capnography will become available from a larger number of vendors at a lower cost point, allowing its integration into platforms that have not seen it widely used. For example, the availability of the volume of expired carbon dioxide and the other volumetric capnographic features as inputs into smart algorithms may lead to improved algorithms such as for the optimization of compressions during CPR.

Early legacy commercial efforts have selected features of the capnogram for classification or as part of a more comprehensive analysis that include a prototype system for respiratory monitoring and a software package for exercise interpretation. Rader [46] described commercial efforts at Perkin–Elmer to show proof of concept of an automated monitoring system, established on a rule- based expert system with 14 time based features per capnogram, to reliably identify 12 different capnographic waveform patterns. The A.I. Series Software Exercise Interpretation Programs (Sensormedics, Yorba Linda, CA) [119] aggregated data, including demographic, respiratory and cardiac measurements from a metabolic cart (e.g. VCO_2) and an ECG stress monitor, and generated a report consisting of a summary table that comprised percent predicted, expected ranges, and annotations and included an if–then rule-based interpretive narrative statement. Other than improved and more robust algorithms described earlier, for both respiratory rate and end-tidal measurements, manufacturer's application of features from the capnogram for prediction and classification has been limited. With respect to commercially available systems, capnographic features have been used, often in combination with other clinical measurements, for indices of pulmonary status, as inputs to an open-loop advisor and a closed-loop system for the management of mechanically ventilated patients, and a computer-assisted sedation system for the delivery of propofol (Table 6). Although not yet available commercially, manufacturers have also explored using features from the capnogram as indicators relating to the effectiveness of the weaning process [120], for classification of the respiratory disorder of a patient [121], and to provide continuous verification of correct placement of endotracheal or supraglottic airway [122].

Researchers continue to expand the use of capnography in novel ways in which classification and prediction can play a part. For example, in a promising small proof of concept study, Brown [43] evaluated the plateau phase from a natural log-transformed capnogram from a mainstream sensor during a forced exhalation maneuver as an indicator of V/Q heterogeneity as measured by CT ($r^2 = 0.49, p = 0.02$). Lukic [123] explored features of the

Table 6 Selected recent commercial applications using capnographic features

Product name/company	Description (510(k)/PMA #, decision date)	Input features	References
Indices			
Integrated Pulmonary Index (IPI) Covidien, Boulder, CO	Index of ventilatory status between 1 and 10 (i.e. worst to best) (K082268, 2/2009)	End-tidal CO_2, respiration rate, oxygen saturation and pulse rate	[103, 104]
Open-loop advisor			
VentAssist, Philips-Respironics, Wallingford, CT	Fuzzy logic based pressure support and ventilation advisor (K103578, 6/2011)	ANN based power of breathing, breathing frequency, tidal volume, ideal body weight, and end-tidal CO_2	[105]
Closed-loop systems			
SmartCare, Drager Medical, Lubeck, Germany	Automatic pressure support adjustment in Evita XL ventilator (K051263, 7/2005)	Respiratory rate, tidal volume and end-tidal CO_2	[106, 107]
INTELLiVENT-ASV mode Hamilton Medical, Bonaduz, Switzerland	Adaptive support ventilation (ASV) with automatic adjustment of oxygenation and ventilation settings (G5 option and standard S1) (not available in US at this time)	Minute volume, tidal volume, and respiratory rate adjusted to reach target end-tidal CO_2 in passive patients and target RR in active patients	[106, 108]
SEDASYS® System, Ethicon Endo-Surgery, Cincinnati, Ohio	Monitors patient parameters and may restrict, suspend, decrease, or stop the propofol infusion based on those parameters. (P080009, 5/2013)	Respiratory rate, end-tidal CO_2 SpO_2, heart rate and blood pressure	[109]

Sources: Respective company websites, FDA 510(k) summaries/PMA summary of safety and effectiveness and cited references

capnogram to characterize the cardiopulmonary effects during controlled human air pollution exposure. Mayer [124] analyzed the capnogram post intravenous delivery of small volume of a sodium bicarbonate solution to detect extravasation during infusion therapy. Studies have also delved into sampling carbon dioxide from alternative sites, such as the tracheal, nasotracheal, and pleural spaces and from the lung via a port in the bronchoscope. Pinskiy [125] described a real-time intubation guidance system consisting of a gas-sampling via a hollow stylet that changes pitch in proportion to the CO_2 level. Other researchers are exploring additional applications, including determining optimal PEEP with the use of phase III slope from volumetric capnogram [126], screening for sleep apnea in acute stroke patients [127], assessing heart failure patients during exercise [128], in systolic heart failure patients, evaluating the prognostic utility of $P_{ET}CO_2$ during rest and exercise [129], and tracking state changes during procedural sedation with patient specific k-means clustering of capnographic features [130].

7 Conclusion

The research, over the last few decades, highlighted in this paper has encompassed the use of features from the time and volumetric capnograms for classification and prediction, and has laid the foundation for future research, new innovations and future commercial implementations. Research efforts should include (a) better leveraging the information available in the capnogram alone and the capnogram in conjunction with other physiological signals (e.g. data fusion) to provide improved diagnosis and therapy, as part of a larger system, (b) incorporating robust, context aware models that can be tuned to specific patients to better understand the current and future clinical state of the patient and (c) leveraging the recent sensor and algorithmic (e.g. machine learning) improvements to enable improved remote monitoring and earlier detection of clinically significant patient changes.

With the growth of electronic health records and the leveraging of that information, the recording of capnographic waveforms, its features and derived metrics, already included in some systems, is anticipated to grow; and use of algorithms with these features as inputs will enhance the identification of artifact and non-physiological data prior to its recording as a permanent record [131]. Due to the revolution in healthcare being driven by the widespread availability of smart phones, high bandwidth cellular networks, and use of social media together with improvements and innovations in sensor technology and design and learning algorithms, applications that have previously been cost-prohibitive, or unimagined are becoming possible and should be actively pursued.

Acknowledgments I would like to thank the following researchers and clinicians for their feedback during the preparation of this paper: John Anderson, Wanqun Bao, Neil Euliano, Julian Goldman, Nik Gravenstein, Mohsen Kazemi, Becky Mieloszyk, Joseph Orr, Adam Seiver, Franck Verschuren, and Kevin Ward.

Compliance with ethical standards

Conflict of interest The author worked previously for Philips Healthcare and currently works as a consultant as Cardiorespiratory Consulting, LLC.

References

1. Barrett WF. On a physical analysis of the human breath. Phil. Mag. 1864; XXVIII:108–21.
2. Rose H. A practical treatise of chemical analysis—Vol. II Quantitative. London: William Tegg and Co.; 1849. p. 534.
3. Wells DA, editor. Year-book of facts in science and art for 1865. Boston: Gould and Lincoln; 1865. p. 245–6.
4. Aiken RS, Clark-Kennedy AE. On the fluctuation in the composition of the alveolar air during the respiratory cycle in muscular exercise. J Physiol. 1928;65:389–411.
5. Jaffe MB. Infrared measurement of carbon dioxide in the human breath: "breathe-through" devices from Tyndall to the present day. Anesth Analg. 2008;107:890–904. doi:10.1213/ane.0b013e31817ee3b3.
6. Jaffe MB. Time and volumetric capnography. In: Ehrenfeld JM, Cannesson M, editors. Monitoring technologies in acute care environments. Berlin: Springer; 2014. p. 179–91.
7. Bellville JW, Seed JC. Respiratory carbon dioxide response curve computer. Science. 1959;130:1079–83.
8. Berengo A, Cutillo A. Single-breath analysis of carbon dioxide concentration records. J Appl Physiol. 1961;16:522–30.
9. Murphy TW. Analogue-digital data processing of respiratory parameters, AFIPS, managing requirements knowledge, international workshop on, managing requirements knowledge, international workshop on 1965, p. 253–57. 1965. doi:10.1109/AFIPS.1965.24.
10. Noe FE. Computer analysis of curves from an infrared CO_2 analyzer and screen-type airflow meter. J Appl Physiol. 1963;18:149–57.
11. Fletcher R. Volumetric capnography: the early days. In: Gravenstein JS, et al., editors. Capnography: clinical aspects. Cambridge: Cambridge University Press; 2004. p. 381–4.
12. Bao W, King P, Zheng J, Smith BE. Expert capnogram analysis. IEEE Eng Med Biol Mag. 1992;11:62–6.
13. Van Genderingen HR, Gravenstein N, van der Aa JJ, Gravenstein JS. Computer-assisted capnogram analysis. J Clin Monit. 1987;3:194–200.
14. Ventzas D. CAPNEX: an expert system for capnography (CO_2 respiration analysis). Trans Institute Measurement Control. 1994;16:233–44.
15. Kelsey JE, Oldham EC, Horvath SM. Expiratory carbon dioxide concentration curve. A test of pulmonary function. Dis Chest. 1962;41:498–503.
16. Smalhout B, Kalenda Z. An atlas of capnography. 2nd ed. Amsterdam: Kerckebosche Zeist Press; 1981.
17. Arsowa S, Schmalisch G, Wauer RR. Techniques and clinical application of capnography in newborn infants and infants. Padiatr Grenzgeb. 1993;31:295–311.
18. Thompson JE, Jaffe MB. Capnographic waveforms in the mechanically ventilated patient. Respir Care. 2005;50:100–8.
19. Technical Staff. A History of Innovation from Novametrix to Philips, Philips Publication. http://www.oem.respironics.com/wp/A_History_of_InnovationFromNovametrix_to_Philips.pdf. 2011. Accessed on 5/29/2015.
20. McSwain SD, Hamel DS, Smith PB, Gentile MA, Srinivasan S, Meliones JN, Cheifetz IM. End-tidal and arterial carbon dioxide measurements correlate across all levels of physiologic dead space. Respir Care. 2010;55:288–93.
21. Levine RL, Wayne MA, Miller CC. End-tidal carbon dioxide and outcome of out-of-hospital cardiac arrest. N Engl J Med. 1997;337:301–6.
22. Wiegand UK, Kurowski V, Giannitsis E, Katus HA, Djonlagic H. Effectiveness of end-tidal carbon dioxide tension for monitoring thrombolytic therapy in acute pulmonary embolism. Crit Care Med. 2000;28:3588–92.
23. You B, Peslin R, Duvivier C, Vu VD, Grilliat JP. Expiratory capnography in asthma: evaluation of various shape indices. Eur Respir J. 1994;7:318–23.
24. Kean TT, Teo AH, Malarvili MB. Feature extraction of capnogram for asthmatic patient. In: Second international conference on computer engineering and applications (ICCEA) p. 251–55. 2010.
25. Herry CL, Townsend D, Green GC, Bravi A, Seely AJE. Segmentation and classification of capnograms: application in respiratory variability analysis. Physiol Meas. 2014;35:2343–58.
26. Bhavani-Shankar K, Philip JH. Defining segments and phases of a time capnogram. Anesth Analg. 2000;91:973–7.
27. Galia F, Brimioulle S, Bonnier F, Vandenbergen N, Dojat M, Vincent JL, Brochard LJ. Use of maximum end-tidal CO_2 values to improve end-tidal CO_2 monitoring accuracy. Respir Care. 2011;56:278–83. doi:10.4187/respcare.00837.
28. Jaffe, MB. What is a valid breath? Methodological Issues. Annual Meeting of the Society for Technology in Anesthesia, abstract 5, 2011.
29. Colman J, Cohen J, Lain D. Smart Alarm Respiratory Analysis (SARA^{TM}) used in capnography to reduce alarms during spontaneous breathing. In: Annual meeting of the Society for Technology in Anesthesia, 2008.
30. Orr JA, Brewer LM, Westenskow DR, Johnson KB. Evaluation of breath rate measurement by capnometry in non-intubated sedated volunteers. In: Anesthesiology, annual meeting of American Society of Anesthesiologists, A1292, 2009.
31. Breen PH, Serina ER, Barker SJ. Measurement of pulmonary CO_2 elimination must exclude inspired CO_2 measured at the capnometer sampling site. J Clin Monit. 1996;12:231–6.
32. Rayburn DB, Fitzpatrick TM, Van Albert SA. Neural network evaluation of slopes from sequential volume segments of expiratory carbon dioxide curves. In: IEEE international conference on neural networks, IEEE world congress on computational intelligence, p. 3530–3, vol. 6. 1994.
33. Tusman G, Scandurra A, Böhm SH, Suarez-Sipmann F, Clara F. Model fitting of volumetric capnograms improves calculations of airway dead space and slope of phase III. J Clin Monit Comput. 2009;23:197–206. doi:10.1007/s10877-009-9182-z.
34. Fletcher R, Jonson B, Cumming G, Brew J. The concept of deadspace with special reference to the single breath test for carbon dioxide. Br J Anaesth. 1981;53:77–88.
35. Fowler WS. Lung function studies; the respiratory dead space. Am J Physiol. 1948;154:405–16.
36. Brewer LM, Orr JA, Pace NL. Anatomic dead space cannot be predicted by body weight. Respir Care. 2008;7:885–91.
37. Tang Y, Turner MJ, Baker AB. Systematic errors and susceptibility to noise of four methods for calculating anatomical dead space from the CO_2 expirogram. Br J Anaesth. 2007;98:828–34.
38. Hjorth Bo, Elema-Schönander AB. EEG analysis based on time domain properties. Electroencephalogr Clin Neurophysiol. 1970;2(2):306–10.
39. Fletcher R, Jonson B. Deadspace and the single breath test for carbon dioxide during anaesthesia and artificial ventilation. Effects of tidal volume and frequency of respiration. Br J Anaesth. 1984;56:109–19.
40. Romero PV, Lucangelo U, Lopez Aguilar J, Fernandez R, Blanch L. Physiologically based indices of volumetric

capnography in patients receiving mechanical ventilation. Eur Respir J. 1997;10:1309–15.
41. Kazemi M. New prognostic index to detect the severity of asthma automatically using signal processing techniques of capnogram. Dissertation. [Malaysia]: Universiti Teknologi. 2013.
42. Pomares Betancourt J, Tangel ML, Yan F, Diaz MO, Portela Otaño AE, Dong F, Hirota K. Segmented wavelet decomposition for capnogram feature extraction in asthma classification. J Adv Comput Intell Intell Inf. 2014;18:480–8.
43. Brown RH, Brooker A, Wise RA, Reynolds C, Loccioni C, Russo A, Risby TH. Forced expiratory capnography and chronic obstructive pulmonary disease (COPD). J Breath Res. 2013;7:017108. doi:10.1088/1752-7155/7/1/017108.
44. Bravi A, Longtin A, Seely AJ. Review and classification of variability analysis techniques with clinical applications. Biomed Eng Online. 2011;10(10):90. doi:10.1186/1475-925X-10-90.
45. Alpaydin E. Introduction to machine learning. 3rd ed. Cambridge: MIT Press; 2014.
46. Flach P. Machine learning: the art and science of algorithms that make sense of data. Cambridge: Cambridge University Press; 2012.
47. Ling CX, Huang J, Zhang H. AUC: a statistically consistent and more discriminating measure than accuracy. Proceedings of the 18th international joint conference on Artificial intelligence (IJCAI'03). San Francisco, CA: Morgan Kaufmann Publishers Inc.; 2003. p. 519–24.
48. Takla G, Petre JH, Doyle DJ, Horibe M, Gopakumaran B. The problem of artifacts in patient monitor data during surgery: a clinical and methodological review. Anesth Analg. 2006;103:1196–204.
49. Rader CD, Crowe VM, Marcot BG. CAPS: a pattern recognition expert system prototype for respiratory and anesthesia monitoring. WESTEX-87. In: Proceedings of the western conference on expert systems, pp. 162–68. 1987.
50. Smith TC, Green A, Hutton P. Recognition of cardiogenic artifact in pediatric capnograms. J Clin Monit. 1994;10:270–5.
51. Bleil M, Opp A, Linder R, Boye S, Gehring H, Hofmann U. Online-classification of capnographic curves using artificial neural networks. In: Vander Sloten J, Verdonck P, Nyssen M, Haueisen J, editors. 4th European conference of the international federation for medical and biological engineering [Internet]. Berlin: Springer. p. 1096–99. 2009. doi:10.1007/978-3-540-89208-3_262.
52. Goldman JM, Dietrich BH. Neural network analysis of physiologic waveforms. Ann Int Conf IEEE Eng Med Biol Soc. 1991;13:1660–1.
53. Navabi-Shirazi MJ. Integration of operating room monitors for development of a smart alarm system. University of Arizona, PhD Dissertation—Electrical and Computer Engineering Department. 1990.
54. Jiang A, King P, Smith B. Information interpretation in a real-time knowledge-based respiratory monitoring system. In: Computing and monitoring in anesthesia and intensive care, p 47–9. 1993.
55. Orr JA, Westenskow DR. A breathing circuit alarm system based on neural networks. J Clin Monit. 1994;10:101–9.
56. Beatty, PCW, Pohlmann A, Dimarki T. Shape-only identification of breathing system failure engineering in medicine and biology society. In: Proceedings of the 22nd annual international conference of the IEEE 2, p. 982–4. 2000.
57. Ahmad F, Stein N, Kondra S, Hofman U, Matz H, Gehring H. Identifying different patterns of capnographic curves on spontaneously breathing patients. Biomedizinische Technik. 2005;50 Suppl v1 Part 2:1541–42.
58. Bleil M. Klassifikation von Kapnogrammen mit Künstlichen Neuronalen Netzen (Classification of the Capnogram with Artificial Neural Nets). Master of Computer Science, Fernuniversität Hagen (University of Hagen, Germany). 2008.
59. Galgóczy G, Mága R, Mándi A. Differential capnographic diagnosis of various ventilation disorders. Pneumonologie. 1972;147:21–8.
60. Vulterini S, Bianco MR, Galmacci G, Pellicciotti L. The capnogram in the study of chronic obstructive lung disease. Ric Clin Lab. 1976;6:149–55.
61. Druck J, Rubio PM, Valley M, Jaffe MB, Yaron M. Evaluation of the slope of phase III from the volumetric capnogram as a non-effort dependent surrogate of peak expiratory flow rate in acute asthma exacerbation. Ann Emerg Med. 2007;50:130.
62. Yaron M, Padyk P, Hutsinpiller M, Cairns CB. Utility of the expiratory capnogram in the assessment of bronchospasm. Ann Emerg Med. 1996;28:403–7.
63. Kazemi M, Malarvili MB. Investigation of capnogram signal characteristics using statistical methods. In: 2012 IEEE EMBS conference on biomedical engineering and sciences (IECBES), p. 343–8. 2012.
64. Addison P. The illustrated wavelet transform handbook: introductory theory and applications in science, engineering, medicine and finance. 1st ed. Boca Raton: CRC Press; 2002.
65. Brown LH, Gough JE, Seim RH. Can quantitative capnometry differentiate between cardiac and obstructive causes of respiratory distress? Chest. 1998;113:323–6.
66. Mieloszyk RJ, Verghese GC, Deitch K, Cooney B, Khalid A, Mirre-Gonzalez MA, Heldt T, Krauss BS. Automated quantitative analysis of capnogram shape for COPD-normal and COPD-CHF classification. IEEE Trans Biomed Eng. 2014;61:2882–90. doi:10.1109/TBME.2014.2332954.
67. Hamrick JL, Hamrick JT, Lee JK, Lee BH, Koehler RC, Shaffner DH. Efficacy of chest compressions directed by end-tidal CO_2 feedback in a pediatric resuscitation model of basic life support. J Am Heart Assoc. 2014;14(3):e000450.
68. Nuckton TJ, Alonso JA, Kallet RH, Daniel BM, Pittet J-F, Eisner MD, Matthay MA. Pulmonary dead-space fraction as a risk factor for death in the acute respiratory distress syndrome. N Engl J Med. 2002;346:1281–6.
69. Hubble CL, Gentile MA, Tripp DS, Craig DM, Meliones JN, Cheifetz IM. Deadspace to tidal volume ratio predicts successful extubation in infants and children. Crit Care Med. 2000;28:2034–40.
70. Akça O. Optimizing the intraoperative management of carbon dioxide concentration. Curr Opin Anaesthesiol. 2006;19:19–25.
71. Cherniack NS, Longobardo GS, Staw I, Heymann M. Dynamics of carbon dioxide stores changes following an alteration in ventilation. J Appl Physiol. 1966;21:785–93.
72. Banner MJ. Partial pressure end-tidal carbon dioxide ($PetCO_2$) monitoring for patients with acute respiratory distress syndrome: effects of physiologic deadspace volume. In: Gravenstein JS, et al., editors. Capnography: clinical aspects. Cambridge: Cambridge University Press; 2004. p. 213–22.
73. Engoren M, Plewa M, O'Hara D, Kline JA. Evaluation of capnography using a genetic algorithm to predict $PaCO_2$. Chest. 2005;127:579–84.
74. Rayburn DB. Non-invasive estimation of arterial blood gases. United States Patent. 5,632,281. May 27, 1997.
75. Chuang ML, Lin IF, Vintch JR, Tien EH. Using statistical techniques to predict dynamic arterial PCO_2 in patients with COPD during maximum exercise. Respir Care. 2012;57:1106–14.
76. Smelt WL, de Lange JJ, Baerts WD, Booij LH. The capnograph, a reliable non-invasive monitor for the detection of pulmonary

embolism of various origin. Acta Anaesthesiol Belg. 1987;38: 217–24.
77. Kline JA, Arunachlam M. Preliminary study of the capnogram waveform area to screen for pulmonary embolism. Ann Emerg Med. 1998;32:289–96.
78. Patel MM, Rayburn DB, Browning JA, Kline JA. Neural network analysis of the volumetric capnogram to detect pulmonary embolism. Chest. 1999;116:1325–32.
79. Kline JA, Kubin AK, Patel MM, Easton EJ, Seupal RA. Alveolar dead space as a predictor of severity of pulmonary embolism. Acad Emerg Med. 2000;7:611–7.
80. Kline JA, Meek S, Boudrow D, Warner D, Colucciello S. Use of the alveolar dead space fraction (Vd/Vt) and plasma D-dimers to exclude acute pulmonary embolism in ambulatory patients. Acad Emerg Med. 1997;4:856–63.
81. Eriksson L, Wollmer P, Olsson CG, Albrechtsson U, Larusdottir H, Nilsson R, Sjögren A, Jonson B. Diagnosis of pulmonary embolism based upon alveolar deadspace analysis. Chest. 1989;96:357–62.
82. Verschuren F, Sanchez O, Righini M, Heinonen E, Le Gal G, Meyer G, Perrier A, Thys F. Volumetric or time-based capnography for excluding pulmonary embolism in outpatients? J Thromb Haemost. 2010;8:60–7. doi:10.1111/j.1538-7836.2009.03667.
83. Rumpf TH, Krizmaric M, Grmec S. Capnometry in suspected pulmonary embolism with positive D-dimer in the field. Crit Care. 2009;13:R196.
84. Kline JA, Hogg MM, Courtney DM, Miller CD, Jones AE, Smithline HA, Klekowski N, Lanier R. D-dimer and exhaled CO_2/O_2 to detect segmental pulmonary embolism in moderate-risk patients. Am J Respir Crit Care Med. 2010;182:669–75.
85. Anderson JA. Embolism. In: Gravenstein JS, et al., editors. Capnography: clinical aspects. Cambridge: Cambridge University Press; 2004. p. 187–98.
86. Verschuren F, Perrier A. Splendors and miseries of expired CO_2 measurement in the suspicion of pulmonary embolism. Crit Care. 2010;14:110. doi:10.1186/cc8838.
87. Manara A, D'hoore W, Thys F. Capnography as a diagnostic tool for pulmonary embolism: a meta-analysis. Ann Emerg Med. 2013;62:584–91. doi:10.1016/j.
88. Affeldt JE, Austin E, Bower AG, Crane MG. Alveolar carbon dioxide levels in acute poliomyelitis. J Appl Physiol. 1956;9: 11–8.
89. Kalenda Z. The capnogram as a guide to the efficacy of cardiac massage. Resuscitation. 1978;6:259–63.
90. White RD, Goodman BW, Svoboda MA. Neurologic recovery following prolonged out-of-hospital cardiac arrest with resuscitation guided by continuous capnography. Mayo Clin Proc. 2011;86:544–8.
91. Touma O, Davies M. The prognostic value of end tidal carbon dioxide during cardiac arrest: a systematic review. Resuscitation. 2013;84:1470–9.
92. Einav S, Bromiker R, Weiniger CF, Matot I. Mathematical modeling for prediction of survival from resuscitation based on computerized continuous capnography: proof of concept. Acad Emerg Med. 2011;18:468–75.
93. Johnson G, Silver A, Freeman GA. Defibrillator display including CPR depth information. United States Patent 8,725,253, May 13, 2014.
94. Joo TH, Stickney RE, Jayne CP, Lank P, O'Hearn P, Hampton DR, Taylor JW, Crone WE, Yerkovich D. Pulse detection apparatus, software, and methods using patient physiological signals. United States Patent 7,917,209, March 29, 2011.
95. Krizmaric M, Verlic M, Stiglic G, Grmec S, Kokol P. Intelligent analysis in predicting outcome of out-of-hospital cardiac arrest. Comput Methods Programs Biomed. 2009;95:S22–32.
96. Shandilya S, Ward K, Kurz M, Najarian K. Non-linear dynamical signal characterization for prediction of defibrillation success through machine learning. BMC Med Inform Decis Mak. 2012;15(12):116.
97. Sheak K, Wiebe DJ, Babaeizadeh S, Yuen TC, Zive D, Owens PC, Edelson DP, Daya M, Idris AH, Abella BS, Leary M. Increasing compression rate and depth positively correlate with end-tidal carbon dioxide during actual CPR performance circulation. (Resuscitation Science Symposium) 130(suppl 2):A15. 2014.
98. Babaeizadeh S, Helfenbein E, Zhou SH. Real-time airway check status indicator. United States Patent Application 20130324872. December 5, 2013.
99. Gonzalez-Castro A, Suarez-Lopez V, Gomez-Marcos V, Gonzalez-Fernandez C, Iglesias-Posadilla D, Buron-Mediavilla J, Rodriguez-Borregan JC, Minambres E, Llorca J. Utility of the dead space fraction (Vd/Vt) as a predictor of extubation success Med. Intensiva. 2011;35:529–38.
100. Rasera CC, Gewehr PM, Domingues AMT. $PETCO_2$ measurement and feature extraction of capnogram signals for extubation outcomes from mechanical ventilation. Physiol Meas. 2015;36: 231–42.
101. Kartal M, Eray O, Rinnert S, Goksu E, Bektas F, Eken C. $ETCO_2$: a predictive tool for excluding metabolic disturbances in nonintubated patients. Am J Emerg Med. 2011;29:65–9.
102. Gravenstein JS, Jaffe MB, Paulus DA, editors. Capnography: clinical aspects. Cambridge: Cambridge University Press; 2004.
103. Taft A, Ronen M, Epps C, Waugh J, Wales R. A Novel Integrated Pulmonary Index (IPI) quantifies heart rate, $Etco_2$, respiratory rate and SpO_2% annual meeting of the American Society of Anesthesiologists, 2008.
104. Berkenstadt H, Ben-Menachem E, Herman A, Dach R. An evaluation of the Integrated Pulmonary Index (IPI) for the detection of respiratory events in sedated patients undergoing colonoscopy. J Clin Monit Comput. 2012;26:177–81.
105. Banner MJ, Euliano NR, Macintyre NR, Layon AJ, Bonett S, Gentile MA, Bshouty Z, Peters C, Gabrielli A. Ventilator advisory system employing load and tolerance strategy recommends appropriate pressure support ventilation settings: multisite validation study. Chest. 2008;133:697–703.
106. Rose L, Schultz MJ, Cardwell CR, Jouvet P, McAuley DF, Blackwood B. Automated versus non-automated weaning for reducing the duration of mechanical ventilation for critically ill adults and children. Cochrane Database Syst Rev. 2014; 10(6): CD009235.
107. Dojat M, Harf A, Touchard D, Lemaire F, Brochard L. Clinical evaluation of a computer-controlled pressure support mode. Am J Respir Crit Care Med. 2000;161(4 Pt 1):1161–6.
108. Lellouche F, Bouchard PA, Simard S, L'Her E, Wysocki M. Evaluation of fully automated ventilation: a randomized controlled study in post-cardiac surgery patients. Intensive Care Med. 2013;39:463–71. doi:10.1007/s00134-012-2799-2.
109. Pambianco DJ, Vargo JJ, Pruitt RE, Hardi R, Martin JF. Computer-assisted personalized sedation for upper endoscopy and colonoscopy: a comparative, multicenter randomized study. Gastrointest Endosc. 2011;73:765–72.
110. Bargeton D. Analysis of capnigram and oxygram in man. Bull Physio-pathol Respir. 1967;3:503–26.
111. Den Buijs JO, Warner L, Chbat NW, Roy TK. Bayesian tracking of a nonlinear model of the capnogram. In: 28th annual international conference of the IEEE engineering in medicine and biology society. EMBS'06, p. 2871–4. 2006.
112. Chbat N, Lord W. Integration of physiological models in medical decision support systems. United States Patent 8,521,556. August 27, 2013.

113. Karlen W, Turner M, Cooke E, Dumont GA, Ansermino JM. CapnoBase: signal database and tools to collect, share and annotate respiratory signals. In: Annual meeting of the society for technology in anesthesia, p. 25. 2010.
114. Orr J, Long C, Brewer LA. CO_2 waveform generator use in evaluating capnometer performance using previously recorded clinical data. In: Annual meeting of the society for technology in anesthesia, 2012.
115. Brochard L, Martin GS, Blanch L, Pelosi P, Belda FJ, Jubran A, Gattinoni L, Mancebo J, Ranieri VM, Richard JC, Gommers D, Vieillard-Baron A, Pesenti A, Jaber S, Stenqvist O, Vincent JL. Clinical review: respiratory monitoring in the ICU—a consensus of 16. Crit Care. 2012;12(16):219. doi:10.1186/cc11146.
116. Sinha P, Flower O, Soni N. Deadspace ventilation: a waste of breath. In: Pinsky MR, Brochard L, Mancebo J, Antonelli M, editors. Applied physiology in intensive care medicine 2: physiological reviews and editorials, 3rd edn. Springer, Berlin, p. 303–14.
117. Suarez-Sipmann F, Bohm SH, Tusman G. Volumetric capnography: the time has come. Curr Opin Crit Care. 2014;20: 333–9.
118. Tusman G, Sipmann FS, Borges JB, Hedenstierna G, Bohm SH. Validation of Bohr dead space measured by volumetric capnography. Intensive Care Med. 2011;37(5):870–4. doi:10.1007/s00134-011-2164-x.
119. Jaffe MB. A computer program for the interpretation of exercise tolerance tests. Comput Methods Programs Biomed. 1986;23: 133–43.
120. Ronen M, Davidpur K, Einav S. Weaning from ventilation using capnography. United States Patent 8,695,596, April 15, 2014.
121. Krauss BS, Hampton DR, Carlebach E. Automated interpretive medical care system and methodology. United States Patent 8,679,029, March 25, 2014.
122. HeartStart MRx with Airway Confirmation Assist Defibrillator/Monitor, Philips Medical Systems, FDA 510(k) Summary (K130153), cleared 3/12/13. http://www.accessdata.fda.gov/scripts/cdrh/cfdocs/cfpmn/pmn.cfm. Accessed 25 July 2015.
123. Lukic KZ, Urch B, Fila M, Faughnan ME, Silverman F. A novel application of capnography during controlled human exposure to air pollution. Biomed Eng Online. 2006;18(5):54.
124. Mayer A, Zholkover A, Keidan I. A functional test for the detection of infusion lines extravasation. In: Conference proceedings on IEEE engineering in medicine and biology society, p. 4180–3. 2014.
125. Pinskiy V, Mori N, Harsh Shah, Dudhat P, Atlas G. Capnography-guided intubation bioengineering conference. In: Proceedings of the IEEE 32nd annual northeast, p. 101–2. 2006.
126. Böhm SH, Maisch S, von Sandersleben A, Thamm O, Passoni I, Martinez Arca J, Tusman G. The effects of lung recruitment on the Phase III slope of volumetric capnography in morbidly obese patients. Anesth Analg. 2009;109:151–9. doi:10.1213/ane.0b013e31819bcbb5.
127. Dziewas R, Hopmann B, Humpert M, Böntert M, Dittrich R, Lüdemann P, Young P, Ringelstein EB, Nabavi DG. Capnography screening for sleep apnea in patients with acute stroke. Neurol Res. 2005;27:83–7.
128. Cundrle I Jr, Somers VK, Johnson BD, Scott CG, Olson LJ. Exercise end-tidal CO_2 predicts central sleep apnea in patients with heart failure. Chest. 2015;147:1566–73.
129. Arena R, Guazzi M, Myers J, Chase P, Bensimhon D, Cahalin LP, Peberdy MA, Ashley E, West E, Forman DE. Prognostic value of capnography during rest and exercise in patients with heart failure. Congest Heart Fail. 2012;18:302–7.
130. Mieloszyk RJ, Guo MG, Verghese GC, Andolfatto G, Heldt T, Krauss BS. Clustering of capnogram features to track state transitions during procedural sedation. In: Engineering in medicine and biology society (EMBC), 37th annual international conference of the IEEE, pp. 1699–702. 2015.
131. Hoare SW, Beatty PC. Automatic artifact identification in anaesthesia patient record keeping: a comparison of techniques. Med Eng Phys. 2000;22:547–53.
132. Romero PV, Rodriguez B, de Oliveira D, Blanch L, Manresa F. Volumetric capnography and chronic obstructive pulmonary disease staging. Int J Chron Obstruct Pulmon Dis. 2007;2:381–91.